Canadian Science Publishing

ARTICLE

From drought to deluge: spatiotemporal variation in migration routing, survival, travel time and floodplain use of an endangered migratory fish

Dalton J. Hance, Russell W. Perry, Adam C. Pope, Arnold J. Ammann, Jason L. Hassrick, and Gabriel Hansen

Abstract: We developed a novel statistical model to relate the daily survival and migration dynamics of an endangered anadromous fish to river flow and water temperature during both extreme drought and severe flooding in an intensively managed river system. Our Bayesian temporally stratified multistate mark–recapture model integrates over unobserved travel times and route transitions to efficiently estimate covariate relationships and includes an adjustment for telemetry tag battery failure. We applied the model to acoustic-tagged juvenile Sacramento River winter-run Chinook salmon (*Oncorhynchus tshawytscha*) and found that survival decreased with decreasing river flows and increased water temperatures. We found that fish were likely to enter a large floodplain during flood conditions and that survival in the floodplain was comparable to the mainstem Sacramento River. Our study demonstrates the response of an endangered anadromous fish population to extreme spatial and temporal variability in habitat accessibility and quality. The general model framework we introduce here can be applied to telemetry of migratory fish through systems with multiple routes to efficiently estimate spatiotemporal variation in survival, travel time, and routing.

Résumé : Nous avons développé un nouveau modèle statistique pour relier la survie quotidienne et la dynamique de la migration d'un poisson anadrome en voie de disparition au débit de la rivière et à la température de l'eau durant des sécheresses et des crues extrêmes dans un réseau hydrographique faisant l'objet d'une gestion intensive. Notre modèle bayésien multi-états de marquage–recapture stratifié dans le temps intègre sur les durées de déplacement et les changements de routes non observés afin d'estimer efficacement des relations entre variables corrélées et il comprend un ajustement pour tenir compte de la défaillance des piles d'étiquettes télémétriques. Nous appliquons le modèle à des saumons chinooks (*Oncorhynchus tshawytscha*) juvéniles de la migration hivernale dans le fleuve Sacramento dotés d'étiquettes acoustiques et constatons que la survie diminue quand les débits diminuent et que les températures de l'eau augmentent. Nous constatons aussi que les poissons sont susceptibles d'entrer dans une grande plaine inondable durant des conditions de crue et que la survie dans la plaine inondable est semblable à la survie dans le bras principal du fleuve Sacramento. L'étude illustre la réaction d'une population de poissons anadromes en voie de disparition à la variabilité spatiale et temporelle extrême de l'accessibilité et de la qualité des habitats. Le cadre général de modélisation que nous présentons peut être appliqué à la télémétrie de poissons migrateurs dans des réseaux comptant des routes multiples, pour l'estimation efficace des variations spatiotemporelles de la survie, de la durée et des routes de déplacement. [Traduit par la Rédaction]

Introduction

Populations of anadromous salmonids evolved in the context of significant spatial and temporal variation in riverine habitat. This variability includes daily, seasonal, and interannual fluctuations in discharge, temperature, and habitat accessibility, each of which may have different impacts on fish survival and behavior across the riverscape. Understanding how critical life stages of anadromous fish respond to riverine environmental conditions over a broad range of spatial and temporal variability is necessary to identify limiting factors to the persistence or recovery of populations as historically extreme hydrologic conditions become more common. Here we use a novel statistical model to track the daily survival and migration dynamics of an endangered anadromous fish in an intensively managed river system in the context of both extreme drought and flooding.

California, USA, is host to distinct climatic conditions as well as a unique population of Chinook salmon (*Oncorhynchus tshawytscha*): the Sacramento River winter-run. Prior to the mid-20th century, winter-run Chinook salmon spawned in the cold spring-fed headwaters of the Sacramento River and emigrated through the Sacramento River and California Delta (the Delta) — a low gradient area of extensive freshwater floodplain and marsh. This fish evolved in the Mediterranean climate of the Sacramento River basin that features a regular pattern of dry summers and wet winters. California's climate has one of the largest interannual variances in precipitation in North America (Dettinger 2016) leading to commensurate interannual variability in migratory and rearing habitat. Winter-run Chinook salmon have persisted through the Sacramento basin's history of both regular droughts and large floods (Earle 1993) and both extremes are expected to become

Received 25 February 2021. Accepted 2 August 2021.

D.J. Hance, R.W. Perry, A.C. Pope, and G. Hansen. US Geological Survey, Western Fisheries Research Center, 5501A Cook-Underwood Road, Cook, WA 98605, USA.
A.J. Ammann. National Marine Fisheries Service, Southwest Fisheries Science Center, 110 McAllister Way, Santa Cruz, CA 95060, USA.
J.L. Hassrick. ICF Jones and Stokes Inc., 980 9th Street Suite 1200, Sacramento, CA 95814, USA.

Corresponding author: Dalton J. Hance (email: dhance@usgs.gov).

more common in future years (Swain et al. 2018). Overlain on this geographical and climatic template of variability is the history of human development of California's land and water. The construction of Shasta and Keswick dams in the 1940s limited spawning habitat for winter-run Chinook salmon to a small cold-water reach downstream of Keswick Dam. These dams are one part of an extensive water storage and delivery system that includes the modified Delta through which juvenile winter-run Chinook salmon must migrate. The Delta consists of a complex network of natural and man-made channels largely disconnected from the historical floodplain and includes channels that are designed, in part, to move water from the Sacramento River to large federal and state pumping stations in the interior Delta (south of the mainstem Sacramento River) that redirect fresh water for agricultural and municipal use. Migrating juvenile salmon may take one of several routes through the Delta and survival and travel times for other runs of Chinook salmon are known to vary among various Delta migration routes and with changing discharge (Perry et al. 2018). One major exception to the history of floodplain disconnection is the Yolo Bypass, a 24 000 ha leveed floodplain located to the west of the city of Sacramento that is designed to divert floodwaters away from urban areas, but which is only flooded in 60% of years (Suddeth Grimm and Lund 2016). Juvenile Chinook salmon rearing in Yolo Bypass have shown enhanced growth and survival (Katz et al. 2017; Sommer et al. 2001; Takata et al. 2017) and actively migrating smolts released directly into Yolo Bypass had survival comparable to fish released into the mainstem Sacramento River (Johnston et al. 2018; Pope et al. 2021). However, the probability that run-of-river Chinook salmon will enter the Yolo Bypass when it is flooding and survival of fish that volitionally enter the Yolo Bypass over a range of flow conditions have not been established.

In this paper, we analyze multiple years of telemetry data on juvenile winter-run Chinook salmon to generate reach-specific estimates of survival, travel time and routing probabilities in relation to daily flows and temperatures in the Delta. Our study evaluates winter-run Chinook salmon survival in the Delta and — when accessible — the Yolo Bypass over a broad range of conditions as it spans a period including both intense drought and extreme flooding. As with similar studies, individual tagged fish were detected imperfectly at telemetry stations spread throughout the study area. To estimate the effect of temporally stratified covariates on survival, individually varying travel times, and imperfect detection, we expanded the temporally stratified Cormack–Jolly–Seber (TSCJS) migration model of Hance et al. (2020) to a multistate context where alternative migration routes represent different "states". This temporally stratified multistate mark–recapture model (TSMS) allowed us to efficiently estimate daily reach-specific travel times, survival, and routing probabilities by integrating over all possible reach-entry times for undetected fish. Our model also incorporated data on tag battery failures to account for the influence of premature tag failure on survival estimates.

Materials and methods

While our TSMS model can be generally applied to any system where individually marked migratory fish can distribute among multiple routes and with varying travel times, in the following sections we describe this model in terms of the specifics of the Sacramento River system. In the first two subsections, we describe the study area and telemetry data collection. In the next two subsections, we detail how telemetry data were condensed into summary statistics and formally define the general TSMS probability model. In the final two subsections, we describe how we parameterized and implemented the model to answer questions about juvenile winter-run Chinook salmon survival and routing in the Delta.

Study area

Although tagged fish were monitored between the upper Sacramento River (river kilometre (rkm) 551) to Golden Gate Bridge (rkm 0), we focused on modelling survival through the Delta, defined here as Yolo Bypass and the channels of the Sacramento River below the city of Knights Landing (rkm 222) downstream as far as Chipps Island (rkm 71) (Fig. 1). We conducted our study in the late winter and early spring of 2014 through 2018, a period encompassing one of the most intense drought water years (2014) in the last 1200 years (Griffin and Anchukaitis 2014) and the record wettest water year (2017) for the northern Sacramento River, which saw extensive flooding including the dramatic partial failure of the Oroville Dam (White et al. 2019). Our model was constructed to estimate reach- and route-specific survival and travel times among five main migration routes: the mainstem Sacramento River (route A), Yolo Bypass (route B), Sutter Slough (route C), Steamboat Slough (route D), and Georgiana Slough (route E) (Fig. 1). We divided the Delta into these distinct routes because these routes have been previously investigated for other runs of Sacramento-origin Chinook salmon and because fish routing and survival through these routes can be affected by resource management actions (Perry et al. 2018). Fish that enter Georgiana Slough have lower survival and greater migration duration than those remaining in the mainstem Sacramento and higher risk of entrainment in state (the State Water Project, SWP) and federal (the Central Valley Project, CVP) water export facilities (Newman and Brandes 2010; Perry et al. 2010). Fish that enter Sutter and Steamboat sloughs avoid the entrance to Georgiana Slough and the predation and entrainment risks of the interior Delta and survive at similar rates to fish that remain in the mainstem Sacramento River (Perry et al. 2018). However, there may be differences between these two routes because of additional channel junctions and potentially more tortuous migrations for fish that enter Sutter Slough as opposed to Steamboat Slough.

Our study also investigates use of the Yolo Bypass by actively migrating Chinook salmon smolts. The Yolo Bypass is an engineered floodplain that is only accessible to downstream migrating fish when the Sacramento River stage exceeds the 10.2 m height of the 2.9 km long Fremont Weir. The Yolo Bypass floodplain contains valuable habitat for rearing (Katz et al. 2017; Takata et al. 2017) and actively migrating juvenile Chinook salmon (Johnston et al. 2018; Pope et al. 2021). Migrating fish that enter the Yolo Bypass avoid entrainment in the interior Delta and telemetered fish released directly into the Yolo Bypass have been demonstrated to have survival similar to those released directly into the Sacramento River (Johnston et al. 2018; Pope et al. 2021). During large flood events, the Yolo Bypass can carry up to four times more water than the mainstem Sacramento River (Suddeth Grimm and Lund 2016). During our study, the Fremont Weir overtopped for 15, 75, and 2 days during the years 2016, 2017, and 2018, respectively, and the discharge of Yolo Bypass during overtopping events ranged from 4% to 280% of the discharge of the mainstem Sacramento River.

Our telemetry network monitored fish at discrete locations throughout the Sacramento River and Delta. Each monitoring station consisted of either two or more acoustic receivers of the juvenile salmon acoustic telemetry system type (JSATS; McMichael et al. 2010). Testing showed detection efficiencies of over 85% at receiver to tag distances of 135 m in average flow and weather conditions (Ammann 2020). The exact brand and location of receivers for monitoring stations varied from year-to-year, but for most locations the same general vicinity was monitored each year. For example, in 2014 receivers for the city of Sacramento were mounted on Tower Bridge (rkm 172), in 2015 they were moved the I-80 bridge (rkm 170) and in the remaining years were present on both bridges. In all these cases, we treated these slight shifts as the same location year-over-year. In other cases, some locations were not monitored in some years because the telemetry network was expanded over the course

Fig. 1. Map of the Sacramento River and Sacramento–San Joaquin Delta showing the location of acoustic telemetry receiving stations (black circles) used to detect migrating acoustic tagged juvenile salmon from 2014 through 2018. These telemetry stations divide the Delta into seventeen discrete reaches, shown as shaded regions labeled by sampling occasions in each migration route (01–10, A–E; see Table 2 and Fig. 2). Yolo Bypass (reaches 03B and 08B) is only accessible when the Fremont weir overtops, which only occurred in 2016, 2017, and 2018. Data and maps © 1999–2021 ESRI. [Colour online.]

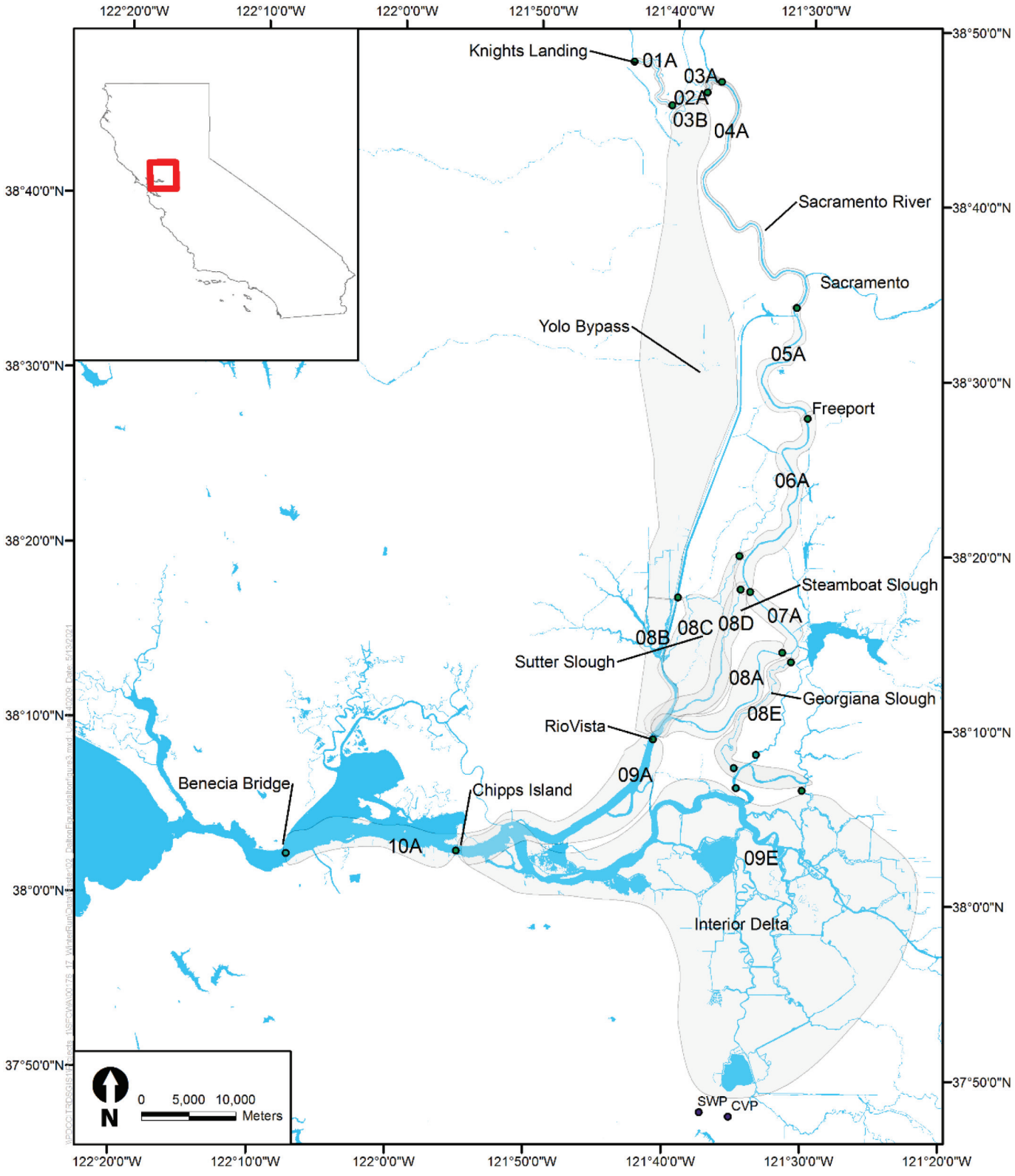

Table 1. Release groups of hatchery-reared winter-run Chinook salmon released in the Sacramento River for evaluation of survival, travel time, and routing.

Year	Release date	Release rkm	*n*	Average weight (SD) (g)	Average length (SD) (mm)
2014	10 Feb.	551.3	358	9.4 (2.4)	94.5 (7.7)
2015	4 Feb.	551.3	249	10.5 (1.9)	99.5 (5.9)
2015	6 Feb.	551.3	318	10.5 (2)	100.5 (6.2)
2016	17 Feb.	540.3	285	9.4 (1.7)	95.5 (5.4)
2016	18 Feb.	540.3	285	9.2 (1.5)	95.4 (4.9)
2017	2 Feb.	551.3	569	9.1 (2.4)	93.1 (7.6)
2018	1 March	540.3	361	16.5 (4.8)	111.9 (10.2)
2018	13 March	540.3	237	10.7 (2.5)	97.5 (6.9)

Note: Release rkm is the river kilometre from the Golden Gate Bridge.

of the study. For example, Chipps Island (rkm 71) was not monitored in 2014 and 2015 and the receivers above (rkm 215) and below Fremont Weir (rkm 210) were only in place for 2017 and 2018. Damage to acoustic receivers also resulted in loss of monitoring capability for at least part of the monitoring period in some locations. For example, receivers in Georgiana Slough near the divergence from the mainstem Sacramento were offline for much of the monitoring period in 2016, 2017, and 2018.

Fish tagging and release

Juvenile winter-run Chinook salmon were obtained from Livingston Stone National Fish Hatchery, a conservation hatchery that sources winter-run Chinook salmon broodstock from a fish trap at the base of Keswick Dam. These natural-origin adults are crossed in the hatchery to maximize genetic diversity. Hatchery juveniles are released at a pre-smolt size to experience some of the same ecological interactions as natural-origin juveniles. Hatchery releases typically coincide with a storm event that is hypothesized to increase survival due to increased river flow and water turbidity resulting in a time window of release from late January to early March (NMFS 2009).

Fish size and the number of acoustic-tagged fish released varied among the five years of this study (Table 1). Acoustic tags weighed 310 mg with dimensions of 10.8 mm × 5.3 mm × 3 mm and were set to a pulse rate interval of 10 seconds (Advanced Telemetry Systems, Isanti, Minnesota). Tags were randomly sampled from a single purchase order and implanted into fish following standard surgical protocols (Liedtke et al. 2012). Mean tag burden (percentage of tag weight/fish weight) by year ranged from 2.9% to 4.1%. With one exception, acoustic tags were surgically implanted into fish 1–3 days prior to their release and one or two releases were conducted at the same location within two days of each other. In 2018, the second release of 237 fish was held for 13 days after tagging to avoid releasing fish in low flow conditions. After the post-surgical holding period in the hatchery, fish were transported to one of two release sites near the city of Redding (rkm 542 or rkm 540). Acoustic tagged fish were released at the same time as non-acoustic tagged hatchery pre-smolts (140 000 to 200 000). Most releases occurred in early February, excepting 2018 when releases occurred in early and mid-March.

Each year, additional acoustic tags (n = 36 in 2014, 32 in 2015 and 30 in 2016–2018) from the same batch of tags as implanted in fish were randomly sampled, activated, and monitored in ambient river water for up to 83 days to estimate each tag's battery life. Each day, the total number of tags still operating and the number of tags that failed were recorded. Based on these data, the Kaplan–Meier (KM) estimator was used to estimate the daily tag survival function for each year. This non-parametric estimator—commonly used in time-to-event analyses, including examples of active-tag mark–recapture in fishes (Cowen and Schwarz 2005)—estimates the probability a tag is still operating at time t.

Summarizing telemetry data as capture histories

Telemetry data were processed in three steps. First, receiver data were screened for false positive detections. Second, screened data were summarized into detection events. Third, individual fish movement patterns were examined to identify potential predation events. False positives were removed using a filter similar to Deng et al. (2017). We grouped the acoustic telemetry data into "detection events" defined as the set of consecutive detections of an individual tag at a given telemetry station uninterrupted by detection at any other telemetry station and separated by less than 60 minutes. Detection events were summarized by receiver location, first and last time of detection. Finally, predation events were identified using the methods of Perry et al. (2018), who adapted the methods of Gibson et al. (2015). Potential predation of tagged smolts was identified using hierarchical clustering of several movement metrics calculated on the acoustic tag detection history of known predators and the study fish. Tag histories of study fish that were grouped with known predators were examined to identify if and when the tag transitioned from smolt-like to predator-like behavior. Any detections after this point were censored (i.e., removed from the data) for the purpose of creating capture histories (Perry et al. 2018).

To create capture histories, general telemetry receiver locations were treated as capture (detection) opportunities and enumerated consistently across years based on the most extensive telemetry network deployed. Reaches were defined as the section of river between subsequent capture opportunities (Fig. 2). The release site was treated as capture opportunity (k) 0 in route (r) A (mainstem Sacramento River) and Knights Landing was capture opportunity 1 in route A (k = 1, r = A). The first possibility for fish to diverge from the Sacramento River was to enter the Yolo Bypass, which could happen at any point along the 2.9 km Fremont Weir, but only when the river stage exceeded 9.8 m. Receivers above (k = 2, r = A) and below (k = 3, r = A) the Fremont Weir bracketed this transition reach. Fish that entered Yolo Bypass had one capture opportunity within the Yolo Bypass near the base of the Toe Drain (rkm 120, k = 4, r = B) before their next opportunity at Rio Vista Bridge in the Sacramento River (rkm 98, k = 9, r = A). Fish that did not enter Yolo Bypass had three more capture opportunities in the mainstem Sacramento before encountering Sutter and Steamboat sloughs (k = 7). This capture opportunity consisted of telemetry receivers in the respective entrances of Sutter (r = C) and Steamboat (r = D) sloughs, as well as receivers just downstream of the junctures within the mainstem Sacramento. Fish that entered Sutter and Steamboat sloughs also had their next capture opportunity at Rio Vista. The final opportunity for divergence from the mainstem Sacramento was into Georgiana Slough (rkm 119, k = 8, r = E). Multiple receivers were maintained in lower Georgiana Slough as well as other channels of the interior Delta including the Mokelumne River. Detections on these receivers were pooled into a single capture opportunity defined as the interior Delta (k = 9, r = E). The penultimate capture opportunity for all routes was at Chipps Island (k = 10, r = A), which marks the entrance of Suisin Bay and the end of the Delta. Because Chipps Island was not monitored in all years, we included a final capture opportunity at Benicia Bridge (k = 11, r = A).

From the records of telemetry station detections we created a 2 × 12 capture history matrix for each individual:

$$\mathbf{C_{i,h}} = \begin{bmatrix} x_{i,h,0} & \cdots & x_{i,h,11} \\ y_{i,h,0} & \cdots & y_{i,h,11} \end{bmatrix}$$

where $x_{i,h,k}$ was the observed state (migration route) of individual h of year i on capture opportunity k if the individual was captured and 0 otherwise. $y_{i,h,k}$ was the observed stratum (day) of individual h of year i on capture opportunity k if the individual was captured and 0 otherwise. In the event of multiple detections at a capture opportunity, we used the timestamp and telemetry

Fig. 2. General schematic of the multistate mark–recapture model with parameters indexed by capture opportunity (k) and by state (migration route, r). Parameters include reach-specific survival probabilities ($\phi_{k,r}$), site-specific detection probabilities ($p_{k,r}$) and routing probabilities from the Sacramento River to route r (ψ_r). The model begins with a release of N_0 acoustic-tagged winter-run Chinook near the city of Redding in each year. The last survival term $\phi^{\dagger}_{10,A}$ is interpreted as the joint probability of surviving from Chipps Island to Benicia Bridge and being detected at Benicia Bridge.

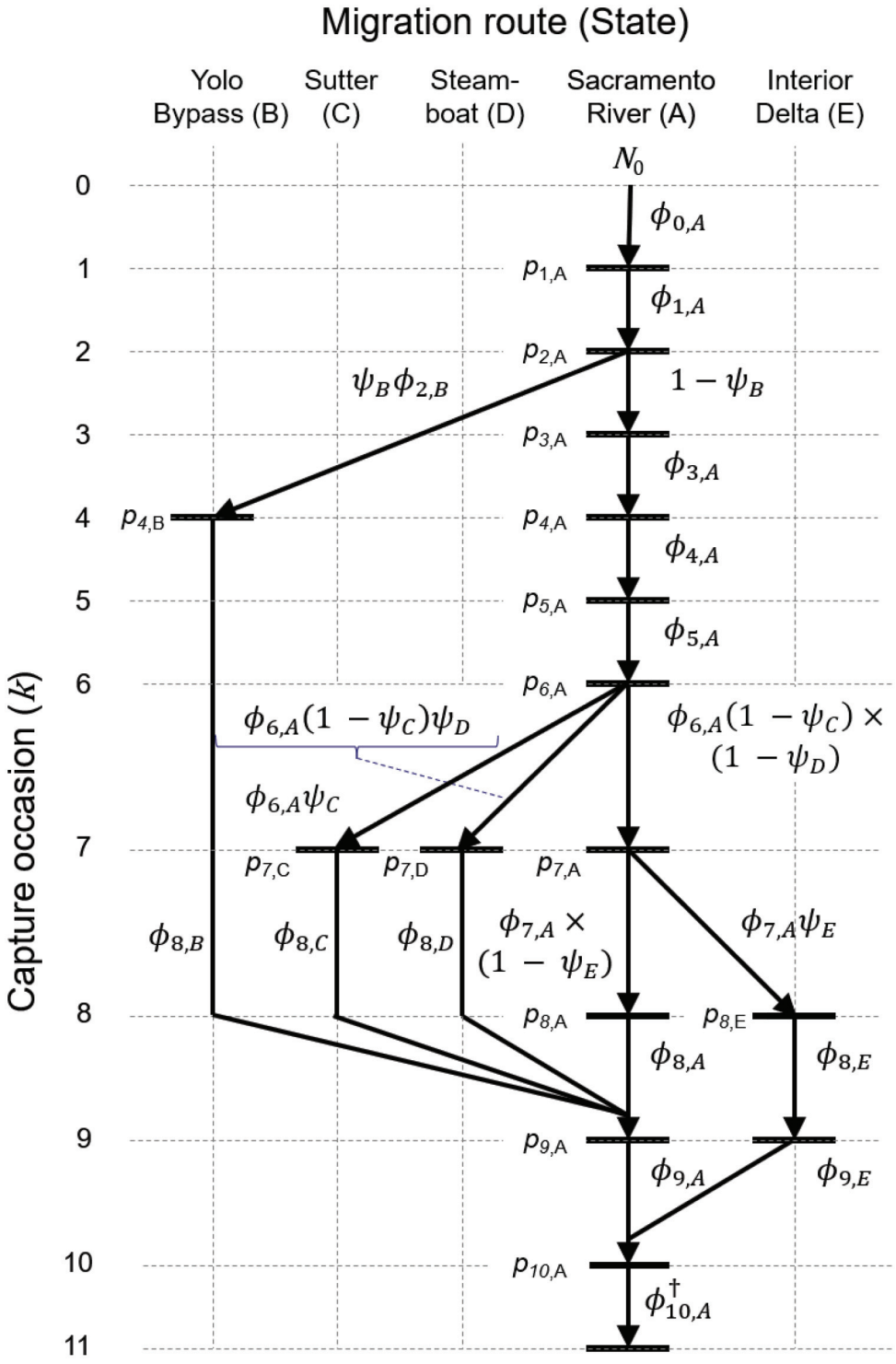

station of the last detection to determine the stratum and state. The capture history matrices were compiled into a set of matrices ($\mathbf{M_{i,j,k,q,r}}$) and a set of vectors ($\boldsymbol{L_{i,k,r}}$) with respective elements summarizing the data as follows: $m_{i,j,k,q,r,s,t}$ was the number of individuals of year i last captured at opportunity j in route q on day s that were next captured at opportunity k in route r on day t; $l_{i,k,r,t}$ was the number of individuals of year i last captured at opportunity k in route r on day t and not captured again. Our model requires setting a maximum number of strata for which fish can be detected, which we denote T. The latest detection of any fish in

our study was 63 days after release, therefore we set $T = 70$ for all years to account for the possibility that fish migrated out after 63 days but were not detected. Thus, $\mathbf{M_{i,j,k,q,r}}$ were each 70×70 matrices of counts of capture pairs with rows corresponding to the s index (departure day) and columns to the t index (arrival day) and $\boldsymbol{L_{i,k,r}}$ were each 70-element vectors of counts of fish last detected on day t.

Mathematical model

To describe the TSMS model, we adopted and expanded upon the notation of the TSCJS model described in Hance et al. (2020). We define the model generally here and describe our specific parameterization in the following section. The TSMS describes a data generating process (Fig. 2) starting with an initial release of fish that survive, arrive over time, are distributed, and detected (captured) at capture opportunities that mark the transition between subsequent downstream reaches and routes. Like most space-for-time mark–recapture models, our model assumes unidirectional movement of fish and does not allow for fish captured at a downstream station to return to an upstream station. Our model is defined in terms of the following parameters:

- $\phi_{i,j,r,s}$ is the probability an individual released in year i that passed capture opportunity j of route r on day s survived to the capture opportunity $j+1$.
- $\alpha_{i,j,r,s,t}$ is the probability of a surviving individual in year i that passed capture opportunity j of route r on day s arriving at capture opportunity $j+1$ on day t, where $\alpha_{i,j,r,s,t} = 0$ for $s > t$, $\alpha_{i,j,r,s,t} > 0$ for $s \leq t$ and $\sum_{t=s}^{T} \alpha_{i,j,r,s,t} = 1$ where T is the final day of the monitoring period.
- $\hat{\delta}_{i,t}$ is the probability an acoustic telemetry tag battery in year i is still active on day t, where $0 \leq \hat{\delta}_t \leq 1$. Here, we used the KM estimate based on time to failure of test-tags in each year and treat as a known parameter.
- $\psi_{i,j,q,r,s}$ and $\psi'_{i,k,q,r,t}$ are the probabilities an individual released in year i entered route r from route q (routing probabilities) on day s or t, respectively. The distinction between ψ and ψ' is that our model allows individuals to transition between routes either immediately after ($\psi_{j,q,r,s}$) or immediately before a capture opportunity ($\psi'_{k,q,r,t}$), where $\psi_{j/k,q,r,s/t} \geq 0$ and $\sum_{r=q}^{R} \psi_{j/k,q,r,s,t} = 1$ and where j/k and s/t indicate using either one variable or the other. Note: in the following we define our model generally, but in practice for each reach only one type of transition should be possible to avoid issues of parameter identifiability.
- $p_{i,k,r,t}$ is the probability an individual released in year i that arrived at capture opportunity k of route r on day t was captured (detected).

Our model integrates over all possible arrival dates and routes for undetected fish using two recursive intermediary parameters (Hance et al. 2020). The first set of recursive terms is used to define the probability of each pair of captures with no other intervening captures. That is, $\lambda_{i,j,k,q,r,s,t}$ is the probability an individual of year i released (or detected) at capture opportunity j in route q on day s survived to capture opportunity k in route r and arrived on day t with an active tag having passed each station between j and k undetected:

$$(1)\quad \lambda_{i,j,k,q,r,s,t} = \sum_{w=1}^{R}\left(\psi_{i,j,q,w,s}\,\phi_{i,j,w,s}\,\alpha_{i,j,w,s,t}\,\psi'_{i,k,w,r,t}\right)\frac{\hat{\delta}_{i,t}}{\hat{\delta}_{i,s}} \quad \text{for } k = j+1 \quad \text{and}$$

$$= \sum_{w=1}^{R}\left[\sum_{u=s}^{T}\lambda_{i,j,k-1,q,w,s,u}\left(1-p_{i,k-1,q,u}\right)\sum_{v=1}^{R}\left(\psi_{i,k-1,w,v,u}\,\phi_{i,k-1,v,u}\,\alpha_{i,k-1,v,u,s,t}\,\psi'_{i,k,v,r,t}\right)\right]\frac{\hat{\delta}_{i,t}}{\hat{\delta}_{i,s}} \quad \text{for } k > j+1$$

The second recursive term defines the probability of not being detected again after the last detection and includes the possibilities that a fish died or the tag battery failed at some point prior to the last capture. That is, $\chi_{i,k,r,t}$ is the probability an individual of year i was last released (or detected) at capture opportunity k in route r on day t. Letting $\chi_{i,K,r,t} = 1$, we have

$$(2)\quad \chi_{i,k,r,t} = \sum_{w=1}^{R}\psi_{i,k,r,w,t}\left(\left(1-\phi_{i,k,w,t}\right) + \phi_{i,k,w,t}\sum_{u=t}^{T}\alpha_{i,k,w,t,u}\left\{\sum_{v=1}^{R}\left[\psi'_{i,k+1,w,v,t}\left(1-p_{i,k+1,v,u}\right)\chi_{i,k+1,v,t}\right]\frac{\hat{\delta}_{i,u}}{\hat{\delta}_{i,t}} + \left(1-\frac{\hat{\delta}_{i,u}}{\hat{\delta}_{i,t}}\right)\right\}\right)$$

Letting $\mathbf{M}$ and $\boldsymbol{L}$ denote the entire set of summary statistic matrices and $\boldsymbol{\theta}$ denote the entire set of parameters, the observed data likelihood can be written as follows:

$$(3)\quad \Pr(\mathbf{M}, \boldsymbol{L}|\boldsymbol{\theta}) \propto \prod_{i=1}^{Y}\prod_{j=0}^{K-1}\prod_{k=j+1}^{K}\prod_{q=1}^{R}\prod_{r=1}^{R}\prod_{s=1}^{T}\prod_{t=s}^{T}\left(\lambda_{i,j,k,q,r,s,t}\,p_{i,k,r,t}\right)^{m_{i,j,k,q,r,s,t}} \times \prod_{i=1}^{Y}\prod_{k=0}^{K}\prod_{r=1}^{R}\prod_{t=1}^{T}\chi_{i,k,r,t}^{l_{i,k,r,t}}$$

Although we defined the model generally, in our application, transitions between routes were highly constrained leading to a limited number of unique combinations of routes and capture occasions (Fig. 2). Given this highly constrained system we only calculated the terms of the likelihood that were possible given the structure of Delta's channel network. Additionally, to avoid identifiability issues due to missing telemetry receivers in 2014 through 2016, travel time from above Fremont Weir to Feather River was parameterized as a single reach rather than two separate reaches.

Parameterization

We parameterized our model to investigate the effects of temporally stratified environmental covariates on survival, travel times, migration routing, and detection probabilities. Based on other Central Valley Chinook salmon stocks (Perry et al. 2018), we hypothesized that discharge would have a positive effect on survival and negative effect on mean travel time and on detection. We also hypothesized that maximum daily water temperatures would have a negative effect on survival (Baker et al. 1995; Notch et al. 2020) and that the ratio of exported water (fresh water removed from the Delta by state and federal pumping facilities) to Delta inflow would have a negative effect on survival for fish that reached the Interior Delta (NMFS 2009). To investigate these hypotheses, we downloaded discharge and temperature data from US Geological Survey (USGS) streamflow gages throughout the Delta (USGS 2020). Flow in the channels of the Delta downstream of Fremont Weir and upstream of Cache Slough are highly correlated (Perry et al. 2018), so for all reaches above Rio Vista and below Vernalis, excluding Yolo Bypass, we used tidally filtered flows at Freeport (USGS Gage 11447650). When the Yolo Bypass is flooding

Table 2. Reaches of the Sacramento River for the temporally stratified multistate mark–recapture model.

Reach	Survival covariates	Notes
00A: Release to Knights Landing	NA	—
01A: Knights Landing to Fremont Weir	Fremont Weir Stage + Freeport Max Temperature	—
02A: Fremont Weir	NA	Above Fremont Weir only monitored in 2017 and 2018; outage from 4–6 April in 2018
03A: Fremont Weir to Feather River	Fremont Weir Stage + Freeport Max Temperature	Below Fremont Weir only monitored in 2017 and 2018; outage from 23–29 March and 4–6 April in 2018
03B: Fremont Weir to Toe Drain	Yolo Bypass Flow + Yolo Bypass Max Temperature	—
04A: Feather River to City of Sacramento	Freeport Flow + Freeport Max Temperature	Feather River receiver outage from 2 Feb. – 26 March in 2017
05A: Sacramento to Freeport	Freeport Flow + Freeport Max Temperature	—
06A: Freeport to Sutter–Steamboat sloughs	Freeport Flow + Freeport Max Temperature	Freeport receiver outage from 4–23 Feb. in 2015
07A: Sutter–Steamboat sloughs to Georgiana Slough	Freeport Flow + Freeport Max Temperature	—
08A: Georgiana Slough to Rio Vista Bridge	Freeport Flow + Freeport Max Temperature	Sacramento River below Georgiana Slough receiver outage for all of 2016, after 13 March in 2017 and from 22 March – 16 April in 2018
08B: Toe Drain to Rio Vista Bridge	Yolo Bypass Flow + Yolo Bypass Max Temperature	Yolo Bypass only monitored in 2016–2018
08C: Sutter Slough to Rio Vista Bridge	Freeport Flow + Freeport Max Temperature	Sutter Slough receiver outage from 2 Feb. – 7 March in 2017
08D: Steamboat Slough to Rio Vista Bridge	Freeport Flow + Freeport Max Temperature	—
08E: Georgiana Slough to Interior Delta	Freeport Flow + Freeport Max Temperature	Georgiana Slough entrance receiver outage for all 2016 and 2017
09A: Rio Vista Bridge to Chipps Island	Rio Vista Flow + Freeport Max Temperature	Chipps Island not monitored in 2014 and 2015
09E: Interior Delta to Chipps Island	Freeport Flow + Freeport Max Temperature + Export/Inflow	Chipps Island not monitored in 2014 and 2015
10A: Chipps Island to Benecia	NA	—

Note: Survival covariates describe which combinations of flow and temperatures variables were used to estimate survival probability. The flow covariate for each reach was also used to model log-mean travel time to the next reach and the probability of detection upon entering the reach. Periods when the entrance to a reach was not monitored due to expansion of the telemetry network over time or due to damage to the acoustic receivers are noted.

there is a large discontinuity in Sacramento River flows upstream and downstream of the Feather River, as well as near the city Rio Vista due to floodwaters reentering the Sacramento River through Cache Slough (Fig. 1). To account for the discontinuities caused by the flooding of the Yolo Bypass, we used Fremont Weir stage height for reaches from Knights Landing to Feather River, and flow in Yolo Bypass (USGS 11453000) for the Yolo Bypass reaches. For reaches below Rio Vista, we used Rio Vista flows (USGS 11455420). We used Freeport flow for the Interior Delta reaches. We only had complete temperature records for the entire study period for the Sacramento River at Freeport and for the Yolo Bypass. Based on exploratory analyses of the partial temperature records from other gaging stations, we opted to use the temperature at Freeport for all reaches except for Yolo Bypass. Lastly, we used the daily ratio of Delta exports to Delta inflow from Dayflow (CNRA 2020) to investigate the effect of water export on survival through the Interior Delta.

While our main objective was to estimate the effect of temporally stratified covariates on survival, travel timing and routing through the Delta, we accounted for fish that may have passed Knights Landing undetected. We modelled survival to and arrival timing at Knights Landing independently for each yearly release, except for 2018 where two releases of fish occurred 11 days apart. This resulted in 6 terms for survival ($\phi_{i,0,1}$), where i refers to each year except for $i = 5,6$, which denotes the first and second releases of 2018, respectively. We modelled arrival timing ($\alpha_{i,0,1,t}$) at Knights Landing using a lognormal kernel with daily lognormal mean-zero process error with separate variances for each year:

$$\alpha_{i,0,1,t} \propto \frac{1}{t-0.5} e^{\left\{ \frac{-[\log(t-0.5)+\mu_{i,0,1}]^2}{2\sigma^2_{i,0,1}} + \epsilon_{i,t} \right\}}$$

where $\mu_{i,0,1}$ is log-mean travel time, and $\sigma^2_{i,0,1}$ is the log-variance of travel time for group i and $\epsilon_{i,t}$ are normally distributed random effects (Hance et al. 2020).

With three exceptions, survival probabilities for all reaches downstream of Knights Landing were modelled as follows:

$$(4) \qquad \text{logit}(\phi_{i,k,r,s}) = \beta_{0,k,r} + \beta_{1,k,r}\text{Flow}_{i,k,r,s} + \beta_{2,k,r}\text{TempMax}_{i,k,r,s}$$

where k and r index the occasion and route of each survival reach, $\beta_{0,k,r}$ is the intercept for logit-survival, $\beta_{1,k,r}$ is the effect of reach-specific flow ($\text{Flow}_{i,k,r,s}$) for day s of year i (Table 2), and $\beta_{2,k,r}$ is the effect of maximum daily temperature ($\text{TempMax}_{i,k,r,s}$) for day s of year i. For the Interior Delta Reach ($k = 9$, $r = \text{E}$), we added an additional term, $+\beta_{3,9,5}\text{E}/I_{i,s}$, which is the effect of the daily export/inflow ratio on survival. For the Sacramento River route reach extending from the receivers above and below Fremont Weir ($k = 2$, $r = \text{A}$) we set survival to 1. This is because receivers were only deployed in these locations for the 2017 and 2018 study years and because when the Fremont Weir is overtopping fish can enter Yolo Bypass at any point along the 2.9 km weir in effect making the entire reach part of Yolo Bypass. Lastly, for the final reach ($k = 10$, $r = \text{A}$), from Chipps Island to Benicia we set survival to a constant across years and days and interpret this parameter as joint survival to and detection at Benicia.

Arrival probabilities at each capture occasion downstream of Knights Landing were modeled using a lognormal kernel with a temporally stratified log-mean travel time and a constant log-variance across years and days for each reach. Enforcing the constraint that arrival probabilities sum to one, we defined the following:

$$\alpha_{i,k,r,s,t} \propto \frac{1}{t-s+0.5} e^{\left\{\frac{-[\log(t-s+0.5)+\mu_{i,k,r,s}]^2}{2\sigma^2_{k,r}}\right\}} \quad (5)$$

and related log-mean travel time for each reach to the daily discharge on the day of entry to the reach:

$$\mu_{i,k,r,s} = \gamma_{0,k,r} + \gamma_{1,k,r}\text{Flow}_{i,k,r,s} \quad (6)$$

We modelled daily routing probabilities based on the flow of the Sacramento River. Fish had four opportunities to diverge from the mainstem Sacramento. The first opportunity was to enter the Yolo Bypass via the Fremont Weir, which was only accessible when the Sacramento River stage at the Fremont Weir exceeded 9.8 m, which only occurred in the 2016, 2017 and 2018 study years. We defined the probability of entering Yolo Bypass as follows:

$$\psi_{B,i,t} = I(\text{Overtop})_{i,t} \times \text{logit}^{-1}(\zeta_{B,0} + \zeta_{B,1}\text{Exceedance}_{i,t}) \quad (7)$$

where $I(\text{Overtop})_{i,t}$ is an indicator variable equals 1 if the Fremont Weir was overtopping and 0 otherwise and $\text{Exceedance}_{i,t}$ is feet above 9.8 m (32 feet). The next three opportunities to diverge from the Sacramento River were always available and for these we used a similar logistic regression formulation:

$$\psi_{X,i,t} = \text{logit}^{-1}(\zeta_{X,0} + \zeta_{X,1}\text{Flow}_{i,t}) \quad (8)$$

to define $\psi_{C,i,t}$, $\psi_{D,i,t}$, $\psi_{E,i,t}$ as the probabilities of entering Sutter, Steamboat, and Georgiana sloughs, respectively, and conditional on not having entered other routes. Here, $\text{Flow}_{i,t}$ is Freeport flow for all three junctions. Because the entrances to Sutter and Steamboat sloughs are fewer than 3 km distant we treated this junction as a three-way divergence and set the probability of entering Sutter Slough as $\psi_{C,i,t}$, the probability of entering Steamboat as $(1 - \psi_{C,i,t})\psi_{D,i,t}$, and the probability of remaining in the Sacramento as $(1 - \psi_{C,i,t})(1 - \psi_{D,i,t})$. Lastly, we set routing probabilities in eq. 3 such that fish in Yolo, Sutter, and Steamboat routes returned to the mainstem Sacramento River at Rio Vista and fish in Interior Delta returned to the mainstem at Chipps Island.

Finally, detection probabilities at all capture occasions in each year were modelled on location-specific flow using the logit-link with year-specific regression coefficients to reflect changes in hydrophone receivers across years:

$$\text{logit}(p_{i,k,r,t}) = \xi_{i,0,k,r} + \xi_{i,1,k,r}\text{Flow}_{i,k,r,t} \quad (9)$$

Detection probabilities during known receiver outages and missing receiver locations had capture probability set to zero for those time periods. We list these receiver outages in Table 2.

To understand the interaction between survival, travel times, and routing probabilities throughout the Delta, we used our model to estimate a set of derived parameters that summarized overall and route specific survival throughout the entire Delta. We used a modified form of the recursive term $\lambda_{i,1,10,1,1,s,t}$ to calculate the probability of a fish departing Knights Landing (j = 1, q = 1) on each day s surviving to Chipps Island (k = 10, r = 1) by removing the $(1 - p)$ terms from each step of the recursion. This allowed us to calculate the overall probability of survival through the Delta for fish passing Knights Landing on each day. We calculated similar summary metrics to estimate overall route specific survivals.

We coded the model in the Stan probabilistic programming language (Carpenter et al. 2017). Flow and temperature covariates were standardized by subtracting the mean and dividing by the standard deviation. We used weakly informative priors for parameters with a small number of more informative priors. Under complex likelihood structures such as ours, weakly informative and informative priors can increase computational efficiency and reduce type I error rates (Lemoine 2019). Priors were chosen using graphical checks to encompass a broad but reasonable range of parameter values given the constraint of the logit transformation and 70-day monitoring period. In general, priors for the terms of the logit-link functions were Student's t distributions with 7 degrees of freedom and standard deviation of 2 for intercept terms and 1 for slope terms. Normal priors were chosen for the terms of μ with mean 0 to 4 and standard deviation of 1 to 2. Half-normal priors with standard deviation of 1 were used for log-variance terms of the travel time distribution. More informative priors were chosen for a handful of locations to mitigate identifiability issues related to travel times. For example, priors for the 2.7 km reach spanning the Fremont Weir were chosen to put more weight on the likelihood of travel times of a day or less. We ran 4 chains with a warmup of 1000 iterations and a sampling of 1000 iterations for a total of 4000 posterior samples. We assessed the adequacy of the fitted model using posterior predictive checks (PPCs). We sampled 1000 draws from the joint posterior distribution and simulated the entire data generating process to create a set of replicated capture histories. We compared the observed data to the distribution of the replicated data for multiple summary statistics: (1) the total number of individuals never recaptured after release in each year, (2) the total number of individuals captured in each route and capture occasion combination in each year, and (3) the total number of individuals captured on each day in each route on each capture occasion.

Results

We verified convergence of the posterior sampler to a stationary distribution through both graphical and statistical summaries. The Gelman–Rubin statistic $(\hat{R})$ for all fundamental parameters of the model was less than 1.01 and the number of effective samples ranged from 1385 to 11 492 (mean 5149). The PPCs indicated adequate, but imperfect fit to the data across multiple dimensions (see online Supplementary material, Figs. S9a–S9s[1]). The observed number of fish never detected after release for each year was within the 90% posterior predictive interval (PPI) for all five years. The observed number detected in each possible state at each capture occasion fell within the 90% PPI for 58 of 67 state-by-occasion combinations. In three cases, the lower bound of the PPI exceeded the observed number of fish detected with a maximum undershoot of 11 (120 observed vs 131 lower bound predicted at k = 10, r = A in 2016). In six cases, the upper bound of the PPI was less than the observed data with a maximum overshoot of 16 (96 observed vs 80 upper bound predicted at k = 11, r = A in 2018). The observed number detected on each day in each state at each capture occasion fell within the 90% PPI for 94% of PPIs that contained nonzero values.

The range of daily flows and temperatures observed during our study were representative of the historical range (Fig. 3). For the months of February through April, flows at Freeport ranged from 142 to 2724 $m^3 \cdot s^{-1}$, respectively less than the 1st percentile and greater than 99th percentile of the 88-year (1930–2018) record. Maximum daily water temperatures at Freeport for the same duration ranged from 9 to 22.7 °C, respectively less than the 7th percentile and greater than 99th percentile of the 57-year (1961–2018) record.

[1]Supplementary data are available with the article at https://doi.org/10.1139/cjfas-2021-0042.

Fig. 3. Daily discharge and daily maximum temperature observed at Freeport during 2014–2018 over a 70-day migration window from the first date of acoustic tagged fish release in each year. The limits of the shaded area represent the daily minimum and maximum record from 88-year (1930–2018) and 57-year (1961–2018) periods of record for discharge and temperature, respectively. [Colour online.]

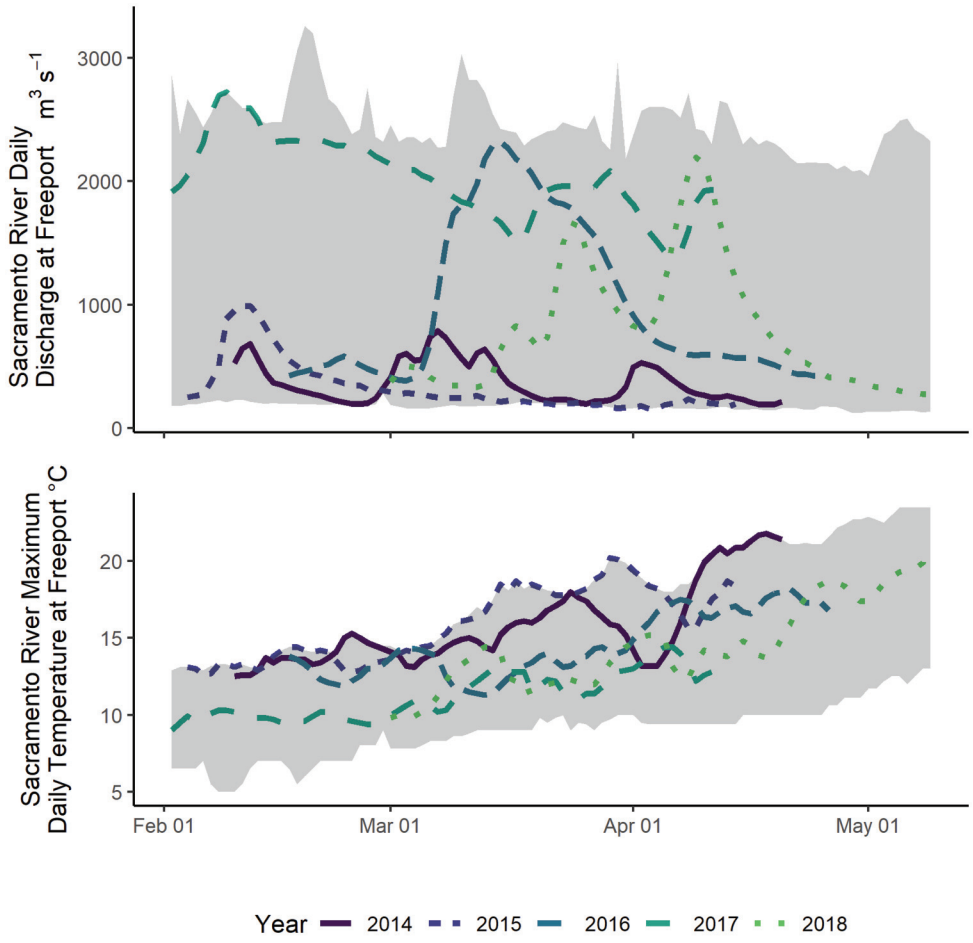

Although we did not estimate covariate relationships for the upper Sacramento River from release to Knights Landing, we observed substantial year-to-year variability in survival and travel time to Knights Landing. Survival probability was highest for this reach in 2016 at 0.58 with a 90% credible interval (CI) of [0.54, 0.62], and lowest for the first release of 2018 at 0.24 (90% CI: [0.20, 0.28]). Fish released during extreme high flows of 2017 had the second highest survival (0.54 with 90% CI: [0.50, 0.58]), but also had much longer travel times with peak arrival day not occurring until 42 days after release (Supplementary Fig. S1[1]). The release group in 2017 also exhibited the earliest tag failure with 10% of tags expected to have failed by day 42 and over 50% by day 66 (Supplementary Fig. S2[1]). This combination of unusually long delay in arrival at Knights Landing and the earliest expected tag failure in 2017 resulted in the largest effect of the tag-life correction for this year.

Baseline survival was relatively high for all reaches below Knights Landing, except for the interior Delta reach. For all reaches outside of the interior Delta, the intercept term for the logistic-link function of survival was greater than zero, which can be interpreted as a baseline survival (i.e., at average discharge and maximum temperature) of greater than 50% (Fig. 4). For these reaches, the posterior mean of baseline survival ranged from 0.69 to greater than 0.99, with all but three reaches greater than 0.85 (03A, 08C, 08D). In contrast, the posterior mean for baseline survival through the Interior Delta was 0.37 (90% CI: [0.17, 0.62]). The posterior mean joint probability of surviving from Chipps Island to Benicia Bridge and being detected was 0.65 (90% CI: [0.61, 0.68]).

Daily discharge tended to have a positive effect on survival in most reaches. The posterior mean was greater than zero for all reaches except for reach 03A, the mainstem Sacramento from below Fremont Weir to the Feather River (Fig. 4). The 90% CI also overlapped zero for reaches of the Yolo Bypass route (reaches 03B and 08B), for Georgiana Slough to the Interior Delta (reach 08E) and for the penultimate reach of the Sacramento Route (09A). The latter two reaches are tidally influenced, which may explain the lack of influence of increasing discharge on survival (Perry et al. 2018). In all remaining reaches, discharge was estimated to have a positive impact on survival (Fig. 5), with the strongest effects apparent in the reaches between the City of Sacramento and Rio Vista (05A through 08A and 08D), which transition from unidirectional flow to bidirectional tidal flow as discharge decreases (Perry et al. 2018). In contrast to the findings of Perry et al. (2018), we found a positive effect of discharge on survival for the Interior Delta to Chipps Island reach (09E). We found no effect for the export/inflow ratio on survival for the Interior Delta reach.

Maximum daily temperature tended to have a negative effect on survival. Although the point estimate for the effect of temperature was negative for all but two reaches, the 90% CI included positive values for all but two reaches (Fig. 4), which means we cannot rule out a small or negligible effect for increasing temperature on survival in these reaches. The two reaches for which temperature had a strong negative effect were both in the northern Delta: reach 03A from the Fremont Weir to Feather River and

Fig. 4. Summary of posterior distributions of parameters for the effects of discharge, maximum daily temperature and export/inflow ratio on survival in each reach of the Sacramento River Delta for acoustic tagged hatchery-reared winter-run Chinook salmon. Parameter estimates are based on the logit-link of survival. Discharge is the centered and scaled reach-specific mean daily discharge. Max Temp is the centered and scaled maximum daily water temperature at Freeport for all reaches except 03B and 08B, which used Yolo Bypass maximum daily water temperature. EI Ratio is the daily ratio of exported water to inflow. [Colour online.]

04A from the Feather River to the City of Sacramento. For these reaches we found that, given a fixed discharge and after accounting for the scaling of the temperature variable, the odds of survival decreased by approximately 70% ($e^{\left(-\frac{4.75}{3.58}\right)} = 0.27$, 90% CI: [0.15, 0.47]) and 45% (0.55 [0.37, 0.81]), respectively for each °C increase in daily maximum temperature (Fig. 6). The combination of observed flow and temperature conditions resulted in declining survival in most reaches by mid-March to early April in all years except 2017 and 2018 (Supplementary Fig. S3[1]).

Daily discharge also affected median travel time. Increasing discharge was associated with decreased travel times in most reaches (Fig. 7). For the first Yolo Bypass reach (03B) and Sutter Slough (08C) the posterior mean was negative but the 90% CI overlapped zero. We found differences in effect of discharge on travel time between Knights Landing and the Feather River between the two parameterizations of the model imposed by the lack of receivers above and below Fremont Weir in 2014 through 2016. In 2014 through 2016, when we modelled travel time from the upstream end of Fremont Weir to Feather River we found a strong negative effect of discharge (stage height at Fremont Weir). This result may have been driven by a small number of long observed travel times between Knights Landing and the Feather River, particularly in 2015, when three fish had observed travel times of 25, 18, and 11 days, respectively. Contrastingly, increased stage height was associated with increased travel times between the downstream end of Fremont Weir and Feather River for 2017 and 2018 (Fig. 8). This likely reflects an alteration to the hydrodynamics of this section of river when the Yolo Bypass overtopped and floodwaters from the Feather River were directed towards and over the Fremont Weir, particularly in 2017. The association of increased discharge with decreased travel times in the remaining reaches correspond with the findings of Perry et al. (2018) for late-fall-run Chinook salmon. We found the longest travel times for fish in the first reach of Yolo Bypass to the base of the Toe Drain with a median travel time at mean flows of 10.1 days (90% CI [7.6, 14.1] days). The second longest travel times were for fish traversing the Interior Delta with a median travel time at mean flows of 6 days (90% CI: [5.4, 6.8] days) to Chipps Island.

Fig. 5. Relationship between discharge and survival probabilities for hatchery-reared winter-run Chinook salmon migrating through the Sacramento River Delta from 2014 through 2018. Lines denote the posterior mean and shaded area the 90% uncertainty interval. The *x* axis extends from the minimum to maximum observed daily value during the study period. The discharge covariate used in the model differed among reaches; for reaches 01A and 03A we used Fremont Weir stage height (note: 1 foot = 30.5 cm), for reaches 03B and 08B we use Yolo Bypass flow, for reaches 09A we used Rio Vista flow, for all other reaches we used tidally averaged flows at Freeport. [Colour online.]

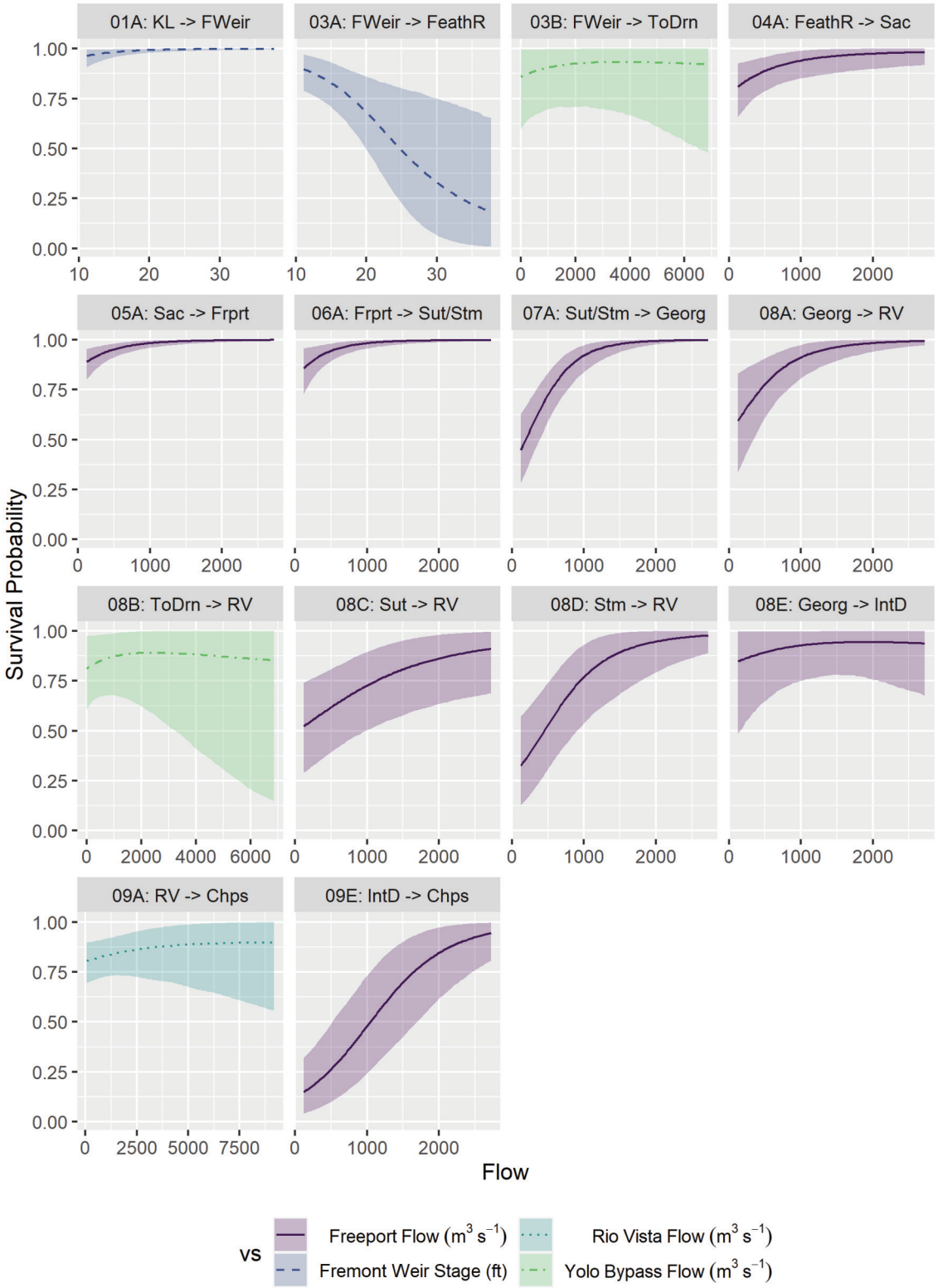

Fig. 6. Relationship between water temperature and survival probabilities for hatchery-reared winter-run Chinook salmon migrating through the Sacramento River Delta from 2014 through 2018. Lines denote the posterior mean and shaded area the 90% uncertainty interval. The *x* axis extends from the minimum to maximum observed daily value during the study period. [Colour online.]

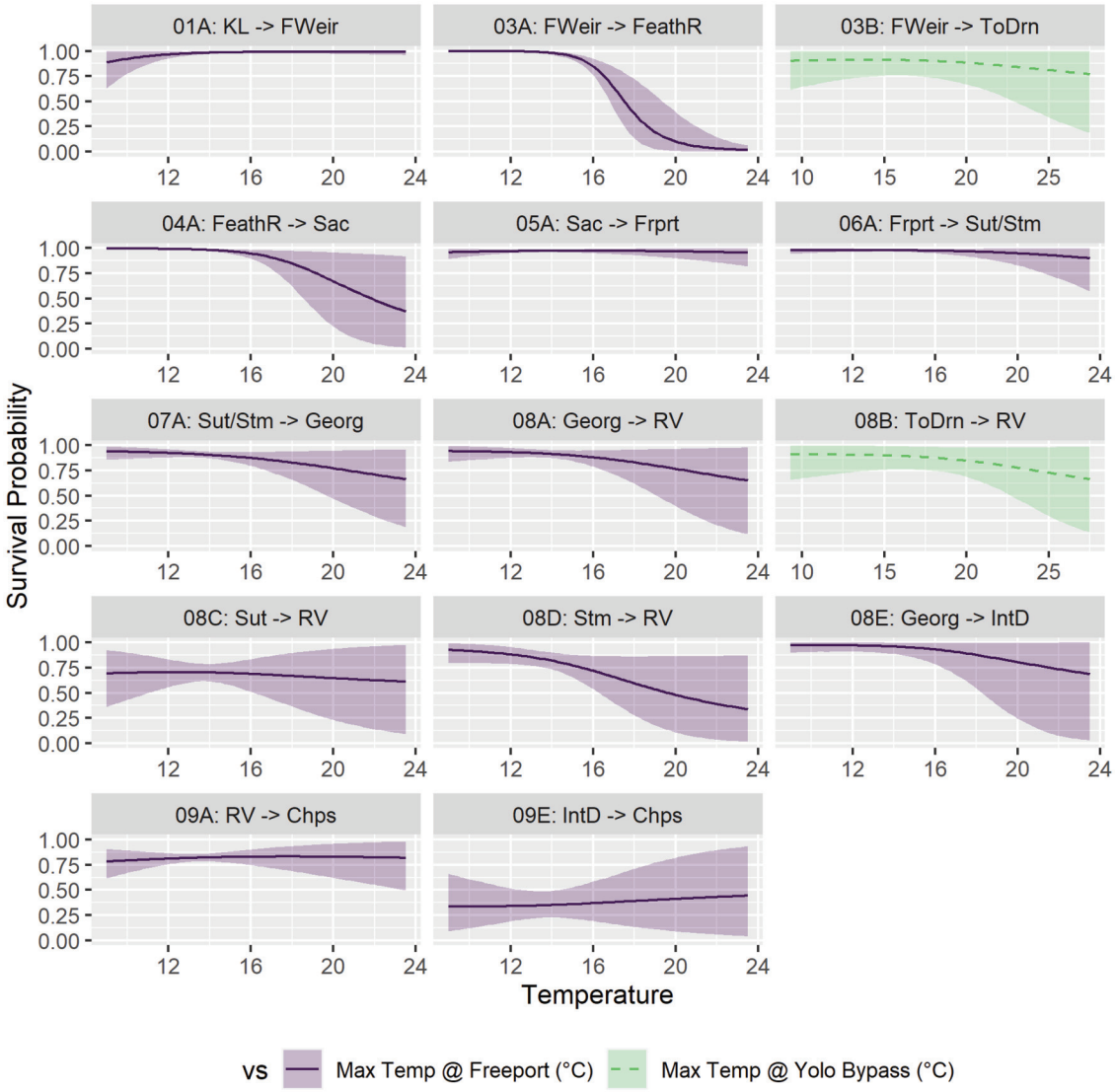

Lastly, we found that routing probability into Yolo Bypass increased with increasing stage height above the Fremont Weir, and routing probability into Steamboat and Georgiana sloughs decreased with increasing Sacramento River flows (Fig. 9). The odds of entering Yolo Bypass (Route B) increased 15-fold (90% CI [7.2, 32.8]-fold) for each foot of river stage above the Fremont Weir with the probability increasing from 0.28 (90% CI: [0.20, 0.36]) at one foot (0.3 m) above to 0.84 (90% CI: [0.76, 0.91]) at two feet (0.6 m) (Fig. 10). We found no effect of increasing discharge on the probability of entering Sutter Slough (Route C) where the posterior mean for the change in the log-odds associated with discharge was near zero (−0.05) and the 90% CI contained both negative and positive values: [−0.3, 0.2]. We found a weak effect of increasing discharge on the odds of entering Steamboat (Route D) and Georgiana sloughs (Route E), where the odds decreased by a factor of 0.74 and 0.80, respectively, for each 734.5 $m^3 \cdot s^{-1}$ increase in Sacramento River discharge. However, the 90% CI for the change in log-odds associated with discharge overlapped zero for Georgiana Slough [−0.5, 0.05]; thus, we cannot rule out a weaker or even no effect of discharge.

Overall survival for winter-run Chinook salmon from Knights Landing to Chipps Island varied within and between years with a general trend of declining survival for fish arriving at Knights Landing later in the year (Fig. 11). The greatest daily overall survival probability occurred during periods when the Fremont Weir was overtopped and Yolo Bypass became available, particularly in 2017 when sustained high flows and relatively cool water temperatures result in daily survivals that remained greater than or equal to the maximum estimated daily survival in all other years throughout the migration period. Overall survival approached 0 for later dates of arrival at Knights Landing for all other years, but the decline began soonest in the drought year of 2015 when overall survival fell below 0.25 by late February. The timing of optimal overall survival in any given year was generally coincident with the highest flows of that year, which occurred relatively early in 2015 (mid-February) and relatively late in 2018 (early-April). However, low discharge alone did not necessarily result in low survival; for example, in 2016 the lowest flows of the study period occurred during late February (Fig. 3) but while overall survival during this period was lower than during the high flows of March it was also

Fig. 7. Summary of posterior distributions of parameters for the effect of discharge on median travel time through each reach of the Sacramento River Delta for acoustic tagged hatchery-reared winter-run Chinook salmon. Parameter estimates are based on the log-mean of lognormally distributed travel times. Discharge is the centered and scaled reach-specific mean daily discharge. [Colour online.]

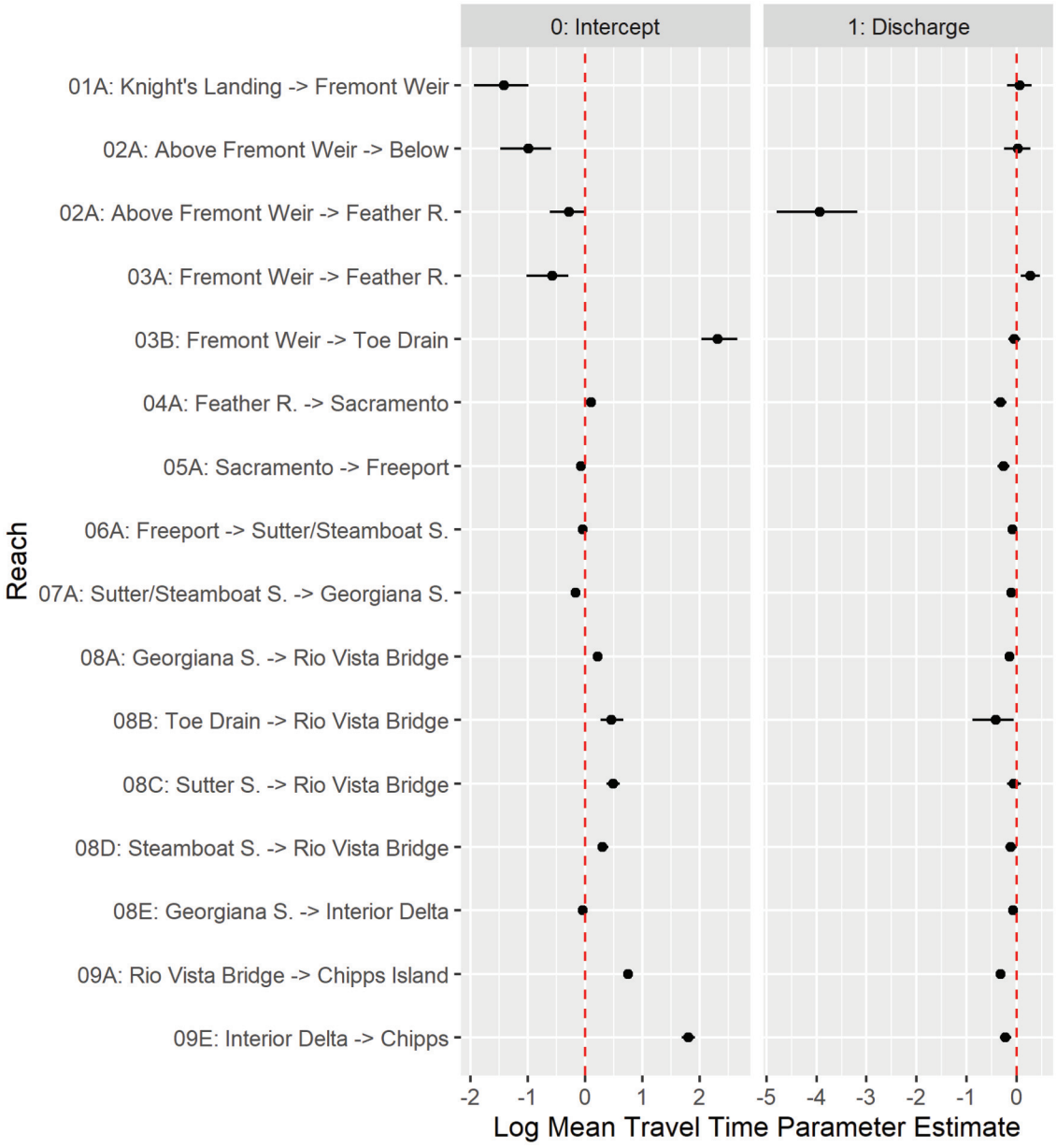

much higher than during the low flow period beginning in April (Fig. 11). This pattern can be attributed to the differences in maximum daily water temperature between early and late lower flow periods. Survival from Knights Landing to Chipps Island by route was similar for all routes except for the Interior Delta, which was lower than other routes for most days in most years, excepting the high flow periods of 2016, 2017, and 2018 when survival through the Interior Delta was comparable to survival through other routes (Supplementary Fig. S8[1]).

Discussion

Sacramento River winter-run Chinook salmon have persisted in a river system characterized by significant daily, seasonal and interannual variability in river flow and water temperature including a history of both extreme droughts and flood. This temporal variability interacts with a spatial variability in migratory habitat including a large floodplain that is currently only accessible during high flows, and several distributary channels including channels that are part of a large municipal and agricultural water export system. Here, we developed a novel statistical mark–recapture model that estimated daily survival, travel-time and routing probabilities throughout the Sacramento River and Delta in the context of extreme drought and record floods. This analysis highlights the extreme spatiotemporal variability in survival and migration dynamics of this endangered salmon population at the southern extent of the species range. Interannual variability in river flows and water temperature during our 5-year study matched the extremes of the long-term record, while seasonal variability influenced reach-specific environmental conditions and the availability of some routes as a migration corridor. This temporal variability influenced how migrating juvenile salmon distributed among the complex branching network of river channels,

Fig. 8. Relationship between discharge and median travel times for hatchery-reared winter-run Chinook salmon migrating through the Sacramento River Delta from 2014 through 2018. Lines denote the posterior mean and shaded area the 90% uncertainty interval. The *x* axis extends from the minimum to maximum observed daily value during the study period. The discharge covariate used in the model differed among reaches; for reaches 01A and 03A we used Fremont Weir stage height (note: 1 foot = 30.5 cm), for reaches 03B and 08B in the Yolo Bypass we use Yolo Bypass flow, for reaches 09A we used Rio Vista flow, for all other reaches we used tidally averaged flows at Freeport. [Colour online.]

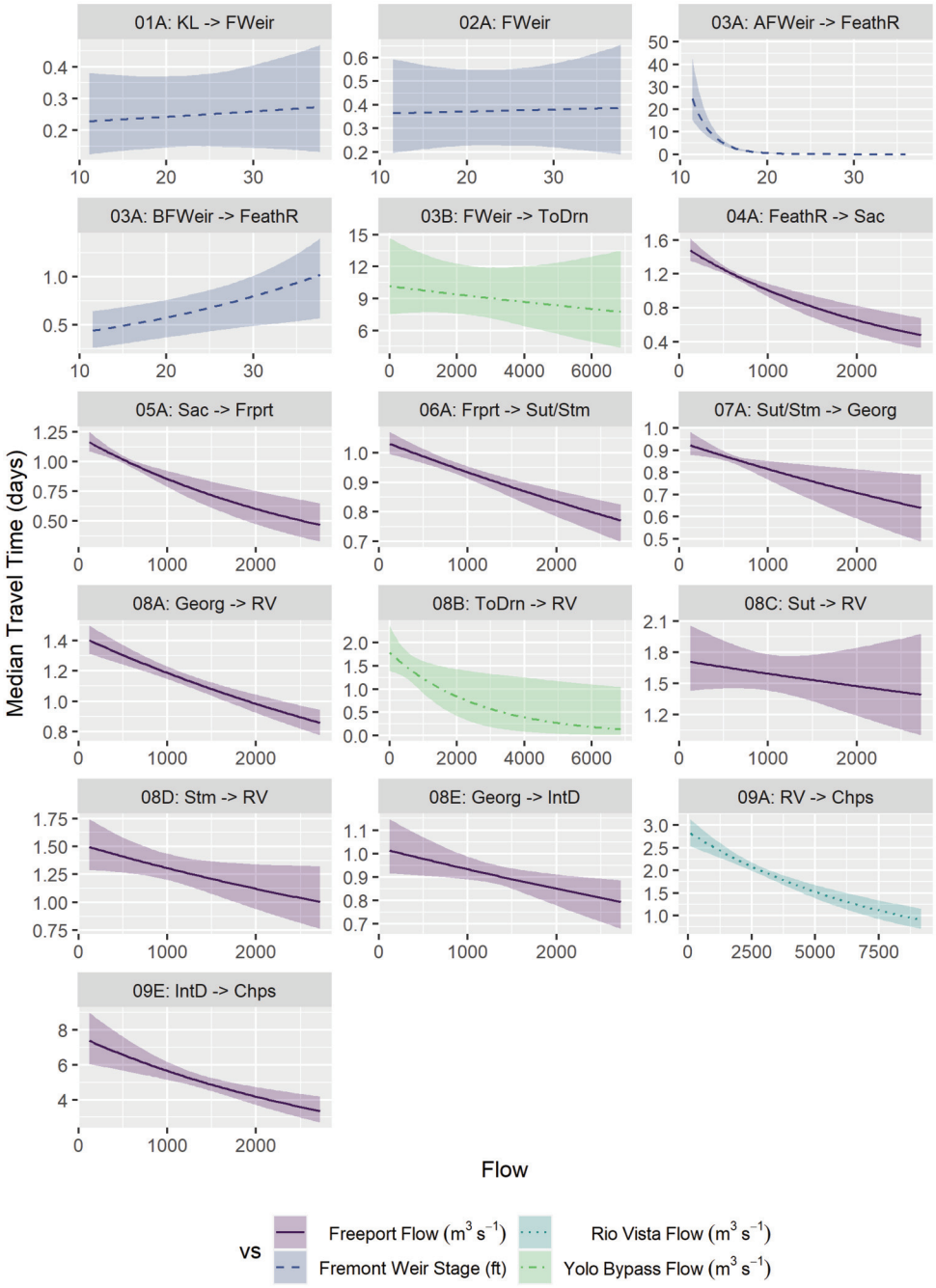

floodplains, and tidal sloughs and the location-specific conditions that ultimately affected their survival. Acoustic telemetry techniques allowed us to track individuals through this spatiotemporal habitat mosaic, and we extended available mark–recapture models to leverage the detailed information contained in these data.

A diversity of populations with different life history characteristics, the so-called portfolio effect, has been shown to support more stable salmon population trajectories over time (Carlson and Satterthwaite 2011; Schindler et al. 2010). Yet the winter-run of Chinook salmon consists of just one population, posing significant risk of extinction for this endangered species. In addition to a diversity of populations, our study illustrates how spatiotemporal variability in available habitat forms another important dimension of the portfolio effect. Use of different migration routes by juvenile salmon "spreads the risk" to the population as a whole from detrimental conditions in a given route. Furthermore, we found that migration times varied significantly among migration routes, spreading out the population not only in space but also in time, which can be important for timing at ocean entry to correspond with marine food availability (Hassrick et al. 2016). The Yolo

Fig. 9. Summary of posterior distributions of parameters for the effect of proportion of flow entering each channel on routing probability at each transition point of major routes through the Sacramento River Delta for acoustic tagged hatchery-reared winter-run Chinook salmon. Parameter estimates are based on the logit-link of routing probability. For Yolo Bypass, discharge is the river stage above the Fremont Weir (equal to 0 when Fremont Weir is not overtopping), for the other three junctions discharge is daily mean Freeport flow. [Colour online.]

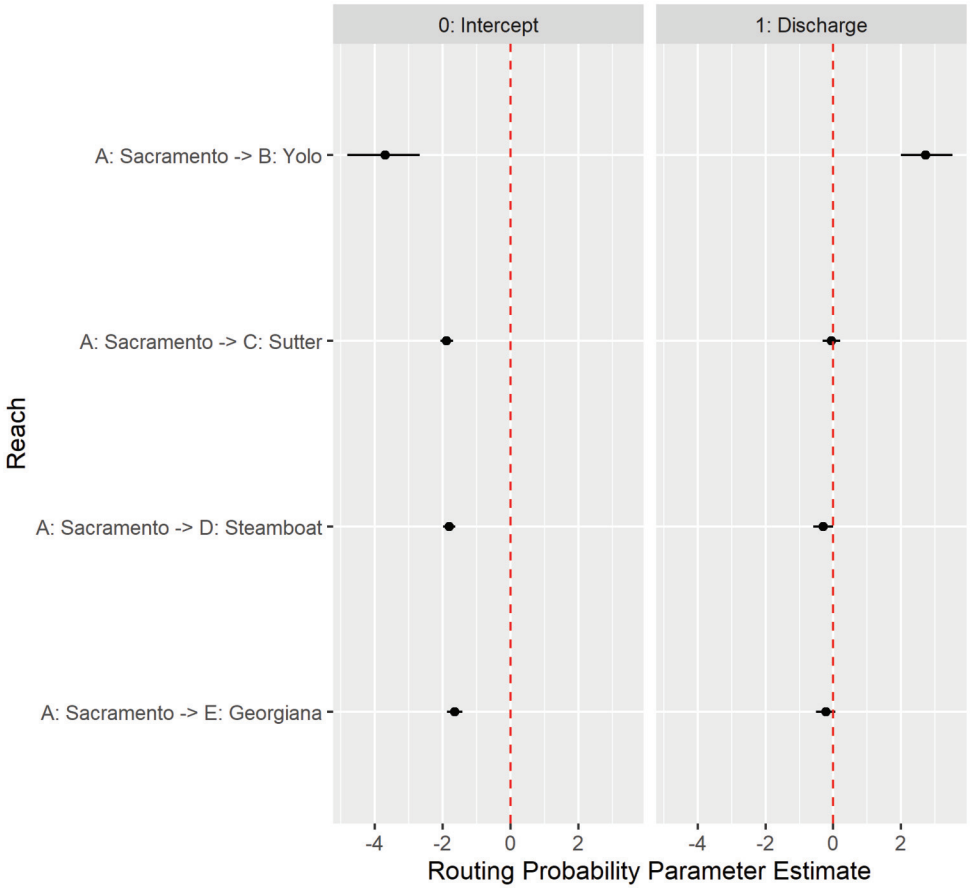

Bypass featured prominently in this spatiotemporal diversity, as juvenile salmon using this route took the longest to migrate through the Delta yet experienced comparable survival to other migration routes and presumably exposed fish to favorable growing conditions (Sommer et al. 2001). Consequently, use of different migration routes with different migration times distributes the arrival timing of individuals in the estuary and nearshore ocean environment. Given our findings that survival depends on conditions that individuals experience at a given location and time, and that ocean entry timing can influence survival to adulthood (Scheuerell et al. 2009), our study illustrates how spatiotemporal variability can arise among individuals within a single population in a way that can act as a buffer against catastrophic events that might otherwise affect the population as a whole.

Our results add to a growing body evidence about the threat of severe drought to the persistence of Sacramento River salmon populations. Our results show that during drought years, winter-run Chinook salmon smolts face a low probability of surviving the later they enter the Delta (defined here as beginning at Knights Landing). Similar to previous studies (Newman and Brandes 2010; Perry et al. 2010), we found that during conditions of low flows and relatively cool water fish that entered the interior Delta had significantly lower survival than those taking other routes. However, during low flow conditions and relatively warmer temperatures we found that survival in all routes was poor. For example, overall survival dropped below 25% for fish arriving at Knights Landing after 1 March in 2015. To the extent this mortality was driven by water temperature, we found the strongest evidence of a correlation with maximum daily water temperature in the upper Delta between Knights Landing and the city of Sacramento. This finding is similar to that of (Singer et al. 2020) who found a survival probability for the reach between the cities of Sacramento and Hood of less than 20% for fall-run and spring-run Chinook salmon smolts released in April of 2014. Thus, our study shows that in addition to the potential impacts of current water delivery infrastructure and operations on winter-run sized Chinook salmon that enter the interior Delta, natural resource management and policymakers should be aware of the potential threats to Chinook salmon of actions that decrease flows and increase water temperatures in the upper Delta (e.g., Perry and Pope 2018). However, it is important to point out that our results only apply to smolt-sized winter-run Chinook salmon that arrive at Knights Landing in the late winter and early spring. In most years, the majority of winter-run Chinook salmon disperse from the upper Sacramento River in November through January (del Rosario et al. 2013), and non-natal rearing including in the Delta is a significant component of winter-run Chinook salmon life histories (Phillis et al. 2018).

Despite poor overall survival conditions in droughts years, our results also demonstrate the adaptability of winter-run Chinook salmon to extreme hydrological conditions. We found that while overall survival through the Delta was generally low during the drought years of 2014 and 2015, specific conditions allowed for brief periods of relatively higher survival. For example, in 2015 fish that arrived at Knights Landing between 8 and 12 February

Fig. 10. Relationship between discharge and routing probabilities for hatchery-reared winter-run Chinook salmon migrating through the Sacramento River Delta from 2014 through 2018. Lines denote the posterior mean and shaded area of the 90% uncertainty interval. The *x* axis extends from the minimum to maximum observed daily value during the study period. (Note: 1 foot = 30.5 cm.) [Colour online.]

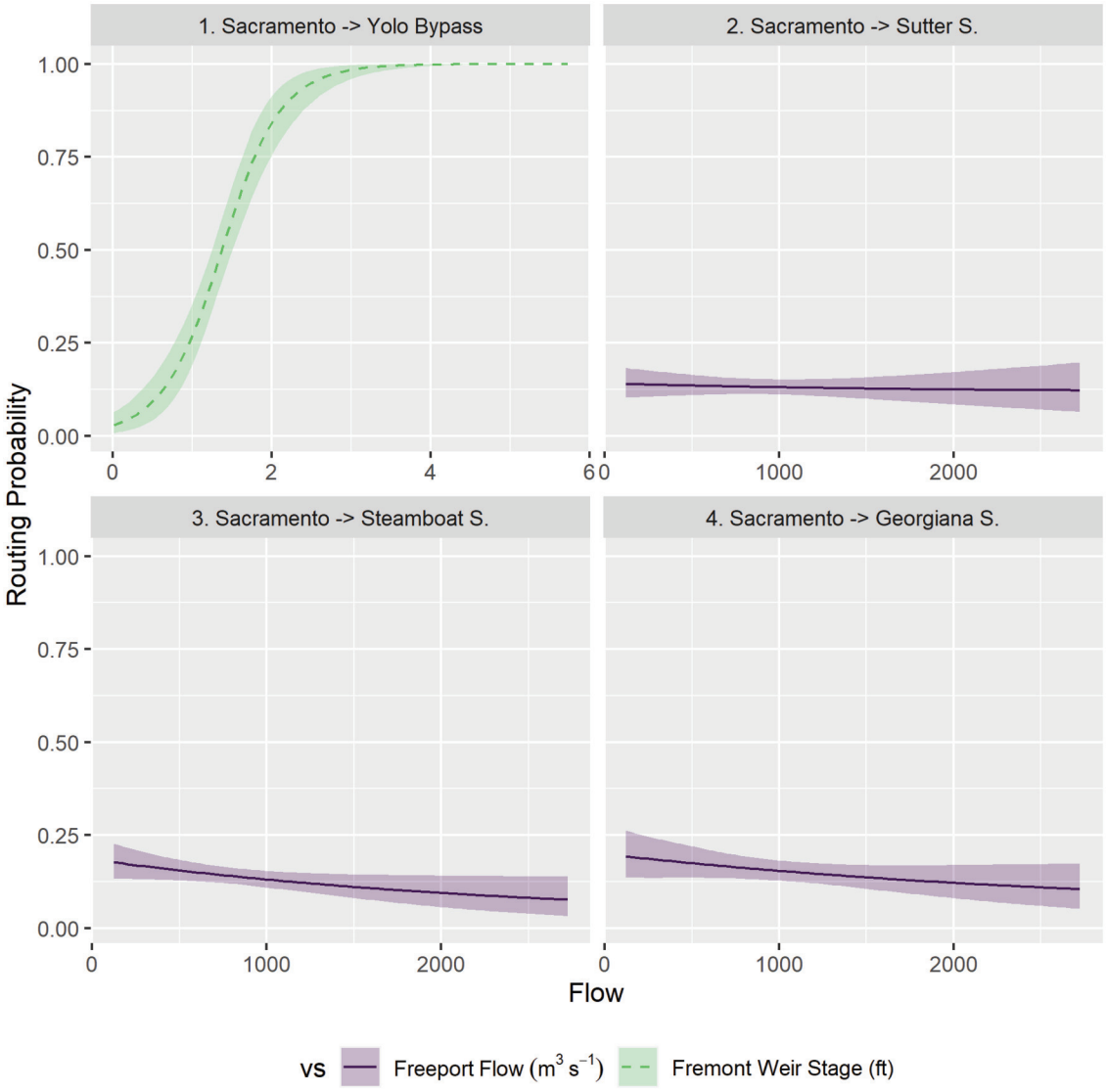

experienced an overall survival through the Delta of between 0.52 and 0.64 (90% uncertainty interval) coincident with a pulse of higher flows. We found that approximately 50% of the release group for that year arrived at Knights Landing in this interval and were able to take advantage of this relatively brief period of improved conditions. In contrast, cumulative Delta survival for fish migrating in 2017 remained high throughout the 70-day monitoring period, and arrival timing at Knights Landing for this year was more protracted with most fish arriving over a two-week period in mid-March. In each year, the peak of arrival timing at Knights Landing for our release groups corresponded with periods of high survival, but with large differences in migration dynamics. If the untagged conservation hatchery fish released at the same time as our study fish responded to the hydrological conditions of these years in a similar manner, then it is possible that winter-run Chinook in 2015 were able to avoid high mortality by shifting migration timing earlier. In doing so, however, these fish may have sacrificed opportunities for growth afforded to the cohort of 2017 (Munsch et al. 2019).

Our study also quantified the probability of entering and surviving through a large intermittently accessible floodplain for an experimental release of Chinook salmon representative of the run-of-river population. We found that winter-run Chinook salmon had a greater probability of entering Yolo Bypass than remaining in the Sacramento River when the Fremont Weir was overtopping by more than 1.25 feet. This value was exceeded for 13 days in 2016 and 56 days in 2017. Fish that entered Yolo Bypass had a probability of survival equivalent to those that remained in the mainstem Sacramento despite a longer residence time. Thus, our findings for volitionally entering smolts confirms experiments where actively migrating smolts were released directly into Yolo Bypass or with experimental releases near Yolo Bypass timed to coincide with a flood event (Johnston et al. 2018; Pope et al. 2021). While these pioneering studies demonstrated the potential value of the Yolo Bypass as a migratory corridor, these studies did not establish to what degree the run-of-river population might use the Yolo Bypass route over a range of flood conditions. The fish in our study were released well upstream of Yolo

Fig. 11. Overall survival through the Sacramento River Delta from Knights Landing to Chipps Island for winter-run Chinook salmon based on day of passage at Knights Landing. Overall survival is calculated by summing through all possible daily survival, arrival day and routing probabilities through downstream reaches. The shaded area represents the 90% uncertainty interval. [Colour online.]

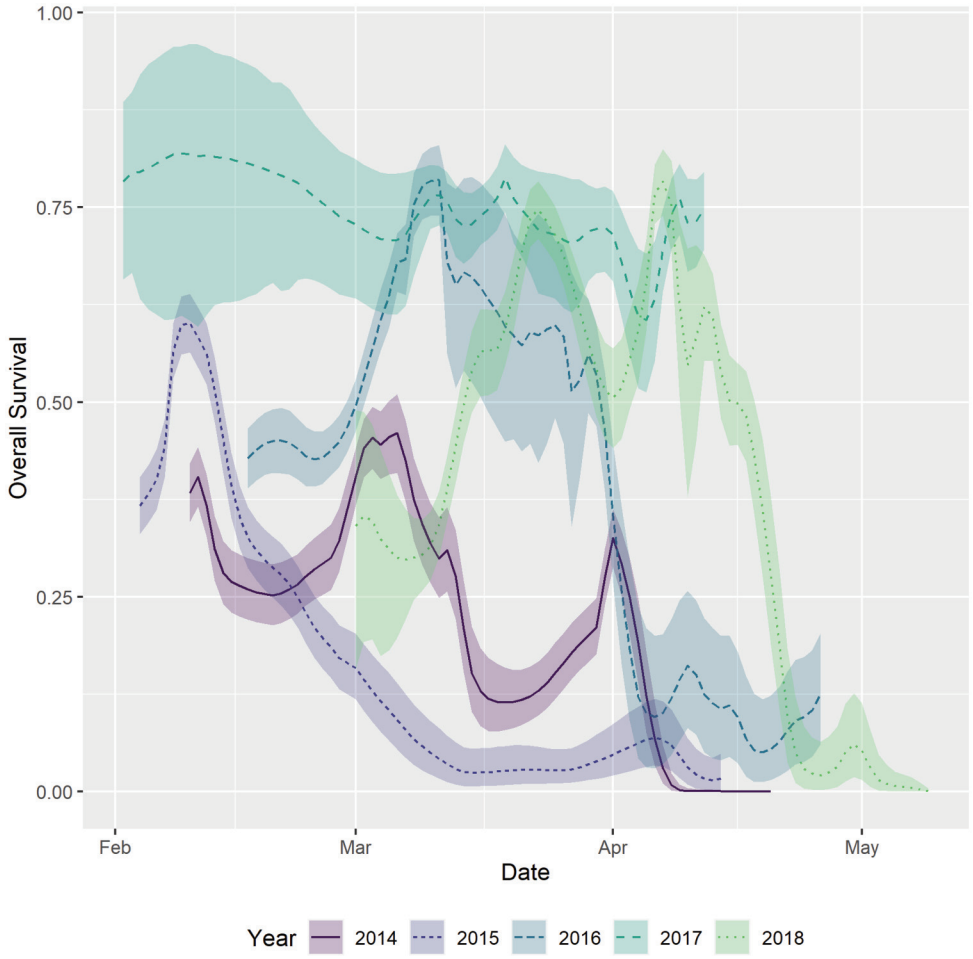

Bypass and so their arrival timing and probability of entering Yolo Bypass are potentially more representative of the run-of-river population. Because juvenile Chinook salmon rearing in Yolo Bypass may experience enhanced growth (Sommer et al. 2001, 2005; Katz et al. 2017; Takata et al. 2017) and avoid channels that enter the interior Delta, our findings demonstrate the importance of improving access to this route for migrating winter-run Chinook salmon.

Although the diverging network channel structure of the Sacramento River and Delta may seem somewhat unique relative to the single migration pathway representative of many other river corridors, our temporally stratified multistate modeling framework can be applied to many situations in which fish use space differentially. Dams on regulated rivers often have multiple passage routes, and lake or nearshore ocean environments may have different migratory pathways among which individuals can be distinguished using telemetry techniques (Holbrook et al. 2015; Skalski et al. 2009). Our analytical framework can link demographic parameters that depend on where fish are in the system of interest (e.g., reach-specific survival, travel times and (or) rates of transition between migratory pathways) to temporally variable covariates. Most other mark–recapture analyses have resorted to summarizing temporal covariates over individuals within release groups, resulting in considerable loss of information. However, Perry et al. (2018) used an approach analogous to ours to estimate the effect of time-varying covariates on juvenile salmon demographics. In their model, they used a complete data likelihood and Monte Carlo simulation to impute travel times and integrate over unobserved covariate values for undetected individuals. In contrast, by discretizing time into temporal strata, our model analytically integrates over all possible strata and covariate values when fish are not detected at a particular sampling occasion. Although both models represent different techniques for tackling the same problem, our model is more computationally efficient because it is implemented in Stan and is better suited to large data sets or spatially complex settings. Our model also offers more flexibility in parameterizing arrival probabilities and accounts for the probability of tag failure. In contrast, our model is unable to account for individual-level covariates (e.g., fish size), whereas the methods of Perry et al. (2018) naturally accommodates individual covariates. Similarly, while we accounted for tag failure using the relatively simple KM estimator the possibility for more robust implementations exists. For example, the terms of eqs. 1 and 2 that account for tag-failure could be modelled using parametric forms such as Weibull or Gompertz curves (Townsend et al. 2006). The model could be further improved by treating tag failure probabilities as parameters to be estimated jointly using eq. 3 combined with an ancillary model for the tag-failure data rather than simply using the tag-failure estimates as known quantities.

While our results are broadly similar to findings for other runs of Chinook salmon migrating through the Sacramento River Delta, some of our findings are in conflict with those of other studies. We identified a weak relationship between river flow and routing at two of the key channel junctions in the Delta and no relationship at a third. Perry et al. (2018) found that routing probability of juvenile late-fall Chinook salmon into Sutter and Steamboat sloughs was positively related to river flow and routing into Georgiana Slough was inversely related to river flow. We found a similar, but weaker relationship at Georgiana Slough, but found that routing into Steamboat was also negatively related to flow. These daily scale relationships are driven by hourly tidal forcing and reverse flows that are dampened as river inflow increases (Perry et al. 2015). In addition, these relationships are important for managed river flows because decreasing river flow increases the proportion of population entering Georgiana Slough, diverting fish to the interior Delta where survival is low and where they may encounter pumping stations. Similarly, Perry et al. (2018) found no effect for river flow on survival through the Interior Delta, whereas in our study we found relatively high survival for fish during the extreme high flows of 2017 and for some of 2016. Thus, the relationships in this study could have potential management implications. We believe that low detection probabilities and loss of monitoring capabilities in some years likely limited our ability to effectively quantify routing relationships that are known to be driven by physical processes. For example, the receivers in Georgiana Slough were lost in two of the five years and in one year had detection probabilities < 0.5 (Supplementary Fig. S6[1]). Although downstream receivers in this route provide information on mean detection probability, the lack of daily detections and associated flows at the time of detection when fish entered Georgiana Slough likely hampered the ability to quantify the effect of flow on routing probability. Finally, our study in contrast to previous studies included reaches further north in the Sacramento Delta, particularly the reaches from Fremont Weir to Feather River. In these reaches we estimated long travel times and relatively low survival over a short distance, particularly during high flows or high temperatures. This area of the Sacramento River includes a major confluence with the Feather River as well as the Sutter and Yolo bypasses. While this area has not previously been identified as a region of high mortality for Chinook salmon (but see Singer et al. 2020), our results show that under certain conditions survival in this area may be quite poor.

Our study sheds light on factors affecting demographic performance of hatchery-origin winter-run Chinook salmon that are intended to support recovery of wild populations. Whether our results can be used to draw inference on the wild population itself depends on the extent to which hatchery-origin fish serve as surrogates for wild fish and the degree of spatiotemporal overlap in the migration dynamics of these two populations. Toward this end, genomic techniques to identify wild juvenile winter-run among mixed-stock catches (Meek et al. 2020) are being integrated into monitoring programs to explicitly estimate annual production of juvenile winter-run leaving the Delta and entering the ocean (Johnson et al. 2017). These efforts should help contextualize our findings and together will provide important insights about management actions needed to recover this imperiled species.

Competing interests statement

The authors declare there are no competing interests.

Contributors' statement

DJH: conceptualization, methodology, formal analysis, software, visualization, writing — original draft. RWP: conceptualization, supervision, project administration, writing — review and editing. ACP: conceptualization, data curation. AJA: investigation, resources, data curation. JLH: investigation, resources, data curation.

Funding statement

This research was supported by the California Department of Fish and Wildlife's Ecosystem Restoration Program (201121366-01), the United States Fish and Wildlife Service's Anadromous Fish Restoration Program (agreement F12PG00194), United States Fish and Wildlife Service (agreement F19PG00040), United States Bureau of Reclamation (agreement R18PG00009) and State Water Contractors, Agreement No. 19WNYD10SWCDELTA.

Data availability statement

The data and R and Stan code necessary to replicate our results are provided as a supplemental file.[1] Data are provided in rds format and include a list of processed capture histories and covariates.

Ethics approval

All work with fish was reviewed and approved by the University of California's Institutional Animal Care and Use Committee (KIERJ1604_A3 and DANNE1905), California Department of Fish and Wildlife permits (SC-13029, CESA MOU ID: Lindley_SRWR CHN_CVSR CHN_CCC Coho_LS_DS_12/31/2018) and National Oceanic and Atmospheric Fisheries Section 10 permits (1112-2, 17299-2M, 17299-3M).

Acknowledgements

Special thanks to Brett Galyean, Bob Null, Kevin Niemela, John Rueth, Albert Duncan, William Hopkins, Kaitlin Gooding, and Travis Webster from the US Fish and Wildlife Service and Livingston Stone National Fish Hatchery for tagging and logistical support. Cyril Michel, Jeremy Notch, Brandon Lehman, and Alex McHuron provided invaluable support in telemetry monitoring. Ramona Zeno provided GIS support. Jacob Krause provided valuable comments on the manuscript. Any use of trade, firm, or product names is for descriptive purposes only and does not imply endorsement by the US Government.

References

Ammann, A.J. 2020. Factors affecting detection probability and range of transmitters and receivers designed for the Juvenile Salmon Acoustic Telemetry System. Environ. Biol. Fishes, **103**: 625–634. doi:10.1007/s10641-020-00987-4.

Baker, P.F., Ligon, F.K., and Speed, T.P. 1995. Estimating the influence of temperature on the survival of chinook salmon smolts (*Oncorhynchus tshawytscha*) migrating through the Sacramento – San Joaquin River Delta of California. Can. J. Fish. Aquat. Sci. **52**(4): 855–863. doi:10.1139/f95-085.

Carlson, S.M., and Satterthwaite, W.H. 2011. Weakened portfolio effect in a collapsed salmon population complex. Can. J. Fish. Aquat. Sci. **68**(9): 1579–1589. doi:10.1139/f2011-084.

Carpenter, B., Gelman, A., Hoffman, M.D., Lee, D., Goodrich, B., Betancourt, M., et al. 2017. Stan: a probabilistic programming language. J. Stat. Softw. **76**: 1–32. doi:10.18637/jss.v076.i0.

CNRA. 2020. Dayflow. California Natural Resources Agency. Available from https://data.cnra.ca.gov/dataset/dayflow [accessed 10 September 2020].

Cowen, L., and Schwarz, C.J. 2005. Capture–recapture studies using radio telemetry with premature radio-tag failure. Biometrics, **61**: 657–664. doi:10.1111/j.1541-0420.2005.00348.x. PMID:16135016.

del Rosario, R.B., Newman, K., Sommer, T., Reece, K., and Vincik, R. 2013. Migration patterns of juvenile winter-run-sized Chinook Salmon (*Oncorhynchus tshawytscha*) through the Sacramento–San Joaquin Delta. San Franc. Estuary Watershed Sci. **11**. doi:10.15447/sfews.2013v11iss1art3.

Deng, Z.D., Martinez, J.J., Li, H., Harnish, R.A., Woodley, C.M., Hughes, J.A., et al. 2017. Comparing the survival rate of juvenile Chinook salmon migrating through hydropower systems using injectable and surgical acoustic transmitters. Sci. Rep. **7**: 42999. doi:10.1038/srep42999. PMID:28220850.

Dettinger, M. 2016. Historical and future relations between large storms and droughts in California. San Franc. Estuary Watershed Sci. **14**: 1. doi:10.15447/sfews.2016v14iss2art1.

Earle, C.J. 1993. Asynchronous droughts in California streamflow as reconstructed from tree rings. Quat. Res. **39**: 290–299. doi:10.1006/qres.1993.1036.

Gibson, A.J.F., Halfyard, E.A., Bradford, R.G., Stokesbury, M.J.W., and Redden, A.M. 2015. Effects of predation on telemetry-based survival estimates: insights from a study on endangered Atlantic salmon smolts. Can. J. Fish. Aquat. Sci. **72**(5): 728–741. doi:10.1139/cjfas-2014-0245.

Griffin, D., and Anchukaitis, K.J. 2014. How unusual is the 2012–2014 California drought? Geophys. Res. Lett. **41**: 9017–9023. doi:10.1002/2014GL062433.

Hance, D.J., Perry, R.W., Plumb, J.M., and Pope, A.C. 2020. A temporally stratified extension of space-for-time Cormack–Jolly–Seber for migratory animals. Biometrics, **76**: 900–912. doi:10.1111/biom.13171.

Hassrick, J.L., Henderson, M.J., Huff, D.D., Sydeman, W.J., Sabal, M.C., Harding, J.A., et al. 2016. Early ocean distribution of juvenile Chinook salmon in an upwelling ecosystem. Fish. Oceanogr. **25**: 133–146. doi:10.1111/fog.12141.

Holbrook, C.M., Bergstedt, R., Adams, N.S., Hatton, T.W., and McLaughlin, R.L. 2015. Fine-scale pathways used by adult sea lampreys during riverine spawning migrations. Trans. Am. Fish. Soc. **144**: 549–562. doi:10.1080/00028487.2015.1017657.

Johnson, R.C., Windell, S., Brandes, P.L., Conrad, J.L., Ferguson, J., Goertler, P.A.L., et al. 2017. Science advancements key to increasing management value of life stage monitoring networks for endangered Sacramento River winter-run Chinook Salmon in California. San Fran. Estuary Watershed Sci. **15**: 1. doi:10.15447/sfews.2017v15iss3art1.

Johnston, M., Espe, M., Klimley, A.P., Sandstrom, P., and Smith, D. 2018. Survival of juvenile Chinook Salmon in the Yolo Bypass and the Lower Sacramento River, California. San Fran. Estuary Watershed Sci. **16**: 4. doi:10.15447/sfews.2018v16iss2art4.

Katz, J.V.E., Jeffres, C., Conrad, J.L., Sommer, T.R., Martinez, J., Brumbaugh, S., et al. 2017. Floodplain farm fields provide novel rearing habitat for Chinook salmon. PloS ONE, **12**: e0177409. doi:10.1371/journal.pone.0177409. PMID:28591141.

Lemoine, N.P. 2019. Moving beyond noninformative priors: why and how to choose weakly informative priors in Bayesian analyses. Oikos, **128**: 912–928. doi:10.1111/oik.05985.

Liedtke, T.L., Beeman, J.W., and Gee, L.P. 2012. A standard operating procedure for the surgical implantation of transmitters in juvenile salmonids. US Geological Survey Open-File Report No. 2012–1267. US Geological Survey, Reston, Va.

McMichael, G.A., Eppard, M.B., Carlson, T.J., Carter, J.A., Ebberts, B.D., Brown, R.S., Weiland, M., Ploskey, G.R., Harnish, R.A., and Deng, Z.D. 2010. The Juvenile Salmon Acoustic Telemetry System: A New Tool. Fisheries, **35**: 9–22. doi:10.1577/1548-8446-35.1.9.

Meek, M.H., Stephens, M.R., Goodbla, A., May, B., and Baerwald, M.R. 2020. Identifying hidden biocomplexity and genomic diversity in Chinook salmon, an imperiled species with a history of anthropogenic influence. Can. J. Fish. Aquat. Sci. **77**(3): 534–547. doi:10.1139/cjfas-2019-0171.

Munsch, S.H., Greene, C.M., Johnson, R.C., Satterthwaite, W.H., Imaki, H., and Brandes, P.L. 2019. Warm, dry winters truncate timing and size distribution of seaward-migrating salmon across a large, regulated watershed. Ecol. Appl. **29**: e01880. doi:10.1002/eap.1880. PMID:30838703.

Newman, K.B., and Brandes, P.L. 2010. Hierarchical modeling of juvenile Chinook salmon survival as a function of Sacramento–San Joaquin delta water exports. N. Am. J. Fish. Manage. **30**: 157–169. doi:10.1577/M07-188.1.

NMFS. 2009. Biological opinion on the long-term Central Valley Project and State Water Project Operation, Criteria, and Plan. National Marine Fisheries Service, Long Beach, Calif.

Notch, J.J., McHuron, A.S., Michel, C.J., Cordoleani, F., Johnson, M., Henderson, M.J., and Ammann, A.J. 2020. Outmigration survival of wild Chinook salmon smolts through the Sacramento River during historic drought and high water conditions. Environ. Biol. Fishes, **103**: 561–576. doi:10.1007/s10641-020-00952-1.

Perry, R.W., and Pope, A.C. 2018. Effects of the proposed California WaterFix North Delta Diversion on survival of juvenile Chinook salmon (*Oncorhynchus tshawytscha*) in the Sacramento-San Joaquin River Delta, northern California. Open-File Report No. 2018–1078. US Geological Survey, Reston, Va.

Perry, R.W., Skalski, J.R., Brandes, P.L., Sandstrom, P.T., Klimley, A.P., Ammann, A., and MacFarlane, B. 2010. Estimating survival and migration route probabilities of juvenile Chinook Salmon in the Sacramento–San Joaquin River Delta. N. Am. J. Fish. Manage. **30**: 142–156. doi:10.1577/M08-200.1.

Perry, R.W., Brandes, P.L., Burau, J.R., Sandstrom, P.T., and Skalski, J.R. 2015. Effect of tides, river flow, and gate operations on entrainment of juvenile salmon into the Interior Sacramento–San Joaquin River Delta. Trans. Am. Fish. Soc. **144**: 445–455. doi:10.1080/00028487.2014.1001038.

Perry, R.W., Pope, A.C., Romine, J.G., Brandes, P.L., Burau, J.R., Blake, A.R., et al. 2018. Flow-mediated effects on travel time, routing, and survival of juvenile Chinook salmon in a spatially complex, tidally forced river delta. Can. J. Fish. Aquat. Sci. **75**(11): 1886–1901. doi:10.1139/cjfas-2017-0310.

Phillis, C.C., Sturrock, A.M., Johnson, R.C., and Weber, P.K. 2018. Endangered winter-run Chinook salmon rely on diverse rearing habitats in a highly altered landscape. Biol. Conserv. **217**: 358–362. doi:10.1016/j.biocon.2017.10.023.

Pope, A.C., Perry, R.W., Harvey, B.N., Hance, D.J., and Hansel, H.C. 2021. Juvenile Chinook salmon survival, travel time, and floodplain use relative to riverine channels in the Sacramento–San Joaquin River Delta. Trans. Am. Fish. Soc. **150**: 38–55. doi:10.1002/tafs.10271.

Scheuerell, M.D., Zabel, R.W., and Sandford, B.P. 2009. Relating juvenile migration timing and survival to adulthood in two species of threatened Pacific salmon (*Oncorhynchus* spp.). J. Appl. Ecol. **46**: 983–990. doi:10.1111/j.1365-2664.2009.01693.x.

Schindler, D.E., Hilborn, R., Chasco, B., Boatright, C.P., Quinn, T.P., Rogers, L.A., and Webster, M.S. 2010. Population diversity and the portfolio effect in an exploited species. Nature, **465**: 609–612. doi:10.1038/nature09060. PMID:20520713.

Singer, G.P., Chapman, E.D., Ammann, A.J., Klimley, A.P., Rypel, A.L., and Fangue, N.A. 2020. Historic drought influences outmigration dynamics of juvenile fall and spring-run Chinook Salmon. Environ. Biol. Fishes, **103**: 543–559. doi:10.1007/s10641-020-00975-8.

Skalski, J.R., Buchanan, R.A., Townsend, R.L., Steig, T.W., and Hemstrom, S. 2009. A multiple-release model to estimate route-specific and dam passage survival at a hydroelectric project. N. Am. J. Fish. Manage. **29**: 670–679. doi:10.1577/M07-227.1.

Sommer, T.R., Nobriga, M.L., Harrell, W.C., Batham, W., and Kimmerer, W.J. 2001. Floodplain rearing of juvenile chinook salmon: evidence of enhanced growth and survival. Can. J. Fish. Aquat. Sci. **58**(2): 325–333. doi:10.1139/f00-245.

Sommer, T.R., Harrell, W.C., and Nobriga, M.L. 2005. Habitat Use and Stranding Risk of Juvenile Chinook Salmon on a Seasonal Floodplain. North Am. J. Fish. Manage. **25**: 1493–1504. doi:10.1577/M04-208.1.

Suddeth Grimm, R., and Lund, J.R. 2016. Multi-purpose optimization for reconciliation ecology on an engineered floodplain — Yolo Bypass, California, USA. San Fran. Estuary Watershed Sci. **14**: 5. doi:10.15447/sfews.2016v14iss1art5.

Swain, D.L., Langenbrunner, B., Neelin, J.D., and Hall, A. 2018. Increasing precipitation volatility in twenty-first-century California. Nat. Clim. Change, **8**: 427–433. doi:10.1038/s41558-018-0140-y.

Takata, L., Sommer, T.R., Louise Conrad, J., and Schreier, B.M. 2017. Rearing and migration of juvenile Chinook salmon (*Oncorhynchus tshawytscha*) in a large river floodplain. Environ. Biol. Fishes, **100**: 1105–1120. doi:10.1007/s10641-017-0631-0.

Townsend, R.L., Skalski, J.R., Dillingham, P., and Steig, T.W. 2006. Correcting bias in survival estimation resulting from tag failure in acoustic and radiotelemetry studies. J. Agric. Biol. Environ. Stat. **11**: 183–196. doi:10.1198/108571106X111323.

USGS. 2020. USGS water data for the Nation: US Geological Survey National Water Information System database. Available from https://doi.org/10.5066/F7P55KJN [accessed 16 December 2020].

White, A.B., Moore, B.J., Gottas, D.J., and Neiman, P.J. 2019. Winter storm conditions leading to excessive runoff above California's Oroville Dam during January and February 2017. Bull. Am. Meteorol. Soc. **100**: 55–70. doi:10.1175/BAMS-D-18-00911.